
IMAGE: A MAP OF THE STARS OF THE ORION CONSTELLATION

Print ISSN: 2631-8490 Online ISSN: 2631-8504

# JournalPreview

London Journal of Research in Science: Natural & Formal

Volume 25 | Issue 15 | Compilation 1.0

Great Britain Journals Press

WWW.JOURNALSPRESS.COM

© COPYRIGHT GREAT BRITAIN JOURNALS PRESS

# JournalPreview

## London Journal of Research in Science: Natural & Formal

This document is a pre-published view of London Journal of Research in Science: Natural & Formal Volume 25, Issue 15 and Compilation 1.0. For any minor changes and updations kindly follow your paper's live editing URL given in given in sent email or get in touch with our support team at support@journalspress.com or visit our website to use live chat support. This is a beta document thus order, content or existence of papers may alter in the published eJournal. You are requested to kindly acknowledge and approve your research paper in this JounalPreview within three days.

THIS IS A CONFIDENTIAL DOCUMENT UNDER A SOLE COPYRIGHT OF GREAT BRITAIN JOURNALS PRESS. IT IS STRICTLY PROHIBITED TO SHARE THIS DOCUMENTS OR ITS COPY IN ANY FORMATE WITH OTHERS OR IN PUBLIC WITHOUT PRIOR PERMISSION OF GREAT BRITAIN JOURNALS PRESS, THIS WILL BE A DIRECT VIOLATION OF TERMS AND CONDITIONS

# Journal Content
## In this Issue

Great Britain Journals Press



©2025 Great Britain Journals Press

Scan to know paper details and
author's profile

# "Quantization of Dark Energy Particles and Sarkar Limit"

*Najmuj Sahadat Sarkar*

## ABSTRACT

In this paper, I have primarily shown how the Dark Energy or Vacuum Energy Field can be quantized. For this purpose, I have taken the help of the Slow Roll Inflation Approximation, in which a special condition is introduced—one that I have named the "Sensitive-φ" condition. Using this as the main framework, we can clearly determine and understand how the scalar field φ varies at an infinitesimal order of magnitude. This paper provides a detailed explanation of the microscopic variations of φ during Slow Roll Inflation, and additionally analyzes the nature and behavior of dark energy particles. It further demonstrates that these particles can also exist in quantized states, since the energy states they occupy correspond to negative energy eigenvalues. These particles have been designated as "Sarkons." All these analytical and mathematical formulations have been presented in my work titled "The Quantization of Dark Energy Particles and the Sarkar Limit.

*Keywords:* sensitive-φ condition, dark energy, cosmological constant, slow roll inflation approximation, hubble parameter, hubble time unit, quantization.

*Classification:* LCC Code: QB981, QC173.6, QC178

*Language:* English

Great Britain Journals Press

LJP Copyright ID: 925615
Print ISSN: 2631-8490
Online ISSN: 2631-8504

London Journal of Research in Science: Natural & Formal

Volume 25 | Issue 15 | Compilation 1.0

© 2025. Najmuj Sahadat Sarkar. This is a research/review paper, distributed under the terms of the Creative Commons Attribution-Noncom-mercial 4.0 Unported License http://creativecommons.org/licenses/by-nc/4.0/), permitting all noncommercial use, distribution, and reproduction in any medium, provided the original work is properly cited.

# "Quantization of Dark Energy Particles and Sarkar Limit"

Najmuj Sahadat Sarkar

## ABSTRACT

*In this paper, I have primarily shown how the Dark Energy or Vacuum Energy Field can be quantized. For this purpose, I have taken the help of the Slow Roll Inflation Approximation, in which a special condition is introduced—one that I have named the "Sensitive-φ" condition. Using this as the main framework, we can clearly determine and understand how the scalar field φ varies at an infinitesimal order of magnitude. This paper provides a detailed explanation of the microscopic variations of φ during Slow Roll Inflation, and additionally analyzes the nature and behavior of dark energy particles. It further demonstrates that these particles can also exist in quantized states, since the energy states they occupy correspond to negative energy eigenvalues. These particles have been designated as "Sarkons." All these analytical and mathematical formulations have been presented in my work titled "The Quantization of Dark Energy Particles and the Sarkar Limit."*

*Keywords:* sensitive-φ condition, dark energy, cosmological constant, slow roll inflation approximation, hubble parameter, hubble time unit, quantization.

*Author:* Mahishadal Raj College, Physics Department, 6295454694, West Bengal, Purba Medinipur.

## I. INTRODUCTION AND CALCULATION

There is no end to scientists' curiosity about our universe. The greatest problem in the universe, especially in theoretical physics, is the problem associated with the cosmological constant. The value we obtain from theory does not match the value determined observationally. My equation has tried, in a particular way, to theoretically analyze this vacuum energy or cosmological constant and determine its nature. In the language of physics I call it the "Sarkar Limit of Inflationary Model". Here the nature of vacuum energy has been analyzed using the "Slow Roll Approximation" or model. Let us begin with the "Friedmann Equation".

The "Friedmann Equation" is used to describe the dynamics of an expanding universe.

$$H^2 = (8\pi G/3)\rho - (kc^2/a^2) + \Lambda/3 \quad (1)$$

Now, according to the "Slow Roll Inflation" model, the total energy density will be:

$$\rho(\varphi) = (1/2)\dot{\varphi}^2 + V(\varphi) \quad (2)$$

$(1/2)\dot{\varphi}^2$ = Kinetic Term of field φ.
$V(\varphi)$ = Potential Term of field φ.

Now, according to "Slow Roll Approximation"

$\dot{\varphi} << 1$, but $\dot{\varphi} > 0$, therefore $\dot{\varphi}^2 \approx 0$ may be considered. On the other hand, the potential energy of the field, that is $V(\varphi) = (1/2)m^2\varphi^2$. Here m is the mass of the field or the mass of the inflation boson. Thus

London Journal of Research in Science: Natural & Formal

©2025 Great Britain Journals Press

simplifying equation (2):

$$\rho(\varphi) = V(\varphi) = (1/2)m^2\varphi^2 \quad (3)$$

Now according to the Friedmann equation (that is, equation (1)), if we simplify slightly, we may set the curvature parameter k = 0. Then equation (1) becomes:

$$H^2 = (8\pi G/3)\rho(\varphi) + \Lambda/3$$

$$3H^2 = 8\pi G\rho(\varphi) + \Lambda$$

$$3H^2 = 4\pi G\varphi^2 m^2 + \Lambda$$

$$\varphi^2 m^2 = (3H^2 - \Lambda) / 4\pi G$$

$$(1/2)\varphi^2 m^2 = (3H^2 - \Lambda) / 8\pi G$$

$$V(\varphi) = (3H^2 - \Lambda) / 8\pi G \quad (4)$$

Another thing we get from "Slow Roll Approximation" is the pressure term P(φ), which is:

$$P(\varphi) = (1/2)\varphi^2 - V(\varphi) \quad (5)$$

Since $\varphi^2 \approx 0$ for slow roll, what remains is:

$$P(\varphi) = -V(\varphi)$$

$$V(\varphi) = -P(\varphi) \quad (6)$$

Now substituting the value of V(φ) from equation (6) into equation (4):

$$P(\varphi) = (\Lambda - 3H^2) / 8\pi G \quad (7)$$

Now according to the mathematical definition of pressure, it is the force per unit area! The type of force depends on the pressure term. Thus:

$$P(\varphi) = F(\varphi) / A \quad (8)$$

Here A is the area. In cosmology we may think of area as the "Horizon Area". That is, $A = d(hor)^2$! Again $d(hor) \approx c^2H^{-2}$. Therefore from equation (8):

$$P(\varphi) = F(\varphi) / d(hor)^2 = F(\varphi) / c^2H^{-2} \quad (9)$$

Here H is the Hubble Parameter, c is the speed of light. In the early moments of the universe, H was extremely large. Another important thing is that in equation (7), Λ represents vacuum energy or the cosmological constant. And G is Newton's gravitational constant. Now substituting the value of P(φ) from equation (7) into equation (9):

$$F(\varphi) / c^2H^{-2} = (\Lambda - 3H^2) / 8\pi G$$

$$F(\varphi) = (c^2 / 8\pi G)[(\Lambda/H^2) - 3] \quad (10)$$


©2025 Great Britain Journals Press

If we compare the scale factor at the beginning of inflation a(initial) and at the end a(final), we get:

$$[a(f)/a(i)] \approx 10^{43}$$

$$a(f) = 10^{43} \times a(i) \tag{11}$$

Equation (11) is mathematically equivalent to e^(H[t(f) – t(i)]). Here t(f) is the time inflation ends, and t(i) is the time inflation begins. Since t(f) > t(i), we can write:

$$[a(f)/a(i)] = e^{(H[t(f) - t(i)])}$$

$$H\Delta t \times \ln(e) = \ln[a(f)/a(i)]$$

$$H \times 10^{-33} \times \ln(2.7) = \ln(10^{43})$$

$$H = 10^{33} \times [\ln(10^{43})/\ln(2.7)]$$

$$H = 10^{35} \text{ km/sec/Mpc} \tag{12}$$

$$\text{Here } \Delta t = [t(f) - t(i)]$$
$$= 10^{-33} - 10^{-36}$$
$$\approx 10^{-33} \text{ seconds.}$$

Substituting the value of H from equation (12) into equation (10):

$$F(\varphi) = (c^2 / 8\pi G)[(\Lambda/H^2) - 3]$$

$$m(d\dot{\varphi}/dt) = (c^2 / 8\pi G)[(\Lambda/10^{70}) - 3] \tag{13}$$

$$m\ddot{\varphi} = (c^2 / 8\pi G)[\Lambda \bullet 10^{-70} - 3]$$

Thus in equation (13) we have $\ddot{\varphi}$ on the left-hand side.According to the condition $\dot{\varphi} << 1$ but $\dot{\varphi} > 0$, $\dot{\varphi}$ varies infinitesimally between 0 and 1. That means we may approximate $\ddot{\varphi} = d\dot{\varphi}/dt$ as an infinitesimal variation. It is not exactly zero, but extremely close to zero. I call this the “Sensitive-φ Condition”. On the left, m denotes the mass of the inflaton boson, the field quanta of the inflation field. $m \approx 10^{12}$ GeV. On the right side of equation (13), the theoretical value of the cosmological constant is $\Lambda \approx 10^{-53}$, but in Planck units $\Lambda \approx 10^{-123} \times l(p)^{-2}$. Here l(p) is the Planck length. In this equation Λ is multiplied by $H^{-2} \approx 10^{-70}$, therefore $\Lambda = 10^{-53} \times 10^{-70}$ or $\Lambda \approx 10^{-123}$ (Hubble Time Unit)! I denote this corrected Λ as Λ(theo). Therefore equation (13) becomes:

$$m\ddot{\varphi} = (c^2 / 8\pi G)[\Lambda \bullet 10^{-70} - 3]$$

$$m\ddot{\varphi} = (c^2 / 8\pi G)[\Lambda(\text{theo}) - 3] \tag{14}$$

Now if Planck’s constant is implemented into equation (14):

$$\hbar = h/2\pi$$

$$2\pi = h/\hbar \tag{15}$$

Thus the present form of equation (14) becomes:



©2025 Great Britain Journals Press

$$m\ddot{\varphi} = (c^2 / 4\pi G) \times (1/2\pi)[\Lambda(theo) - 3]$$

$$m\ddot{\varphi} = (c^2 / 4\pi G) \times (\hbar/h) \times [\Lambda(theo) - 3]$$

$$m\ddot{\varphi} = (c^2 / 2Gh) \times [(1/2)\hbar \times \Lambda(theo) - (3/2)\hbar]$$

$$m\ddot{\varphi} = (c^2 / 4\pi G\hbar) \times [(1/2)\hbar \times \Lambda(theo) - (3/2)\hbar]$$

Therefore:

$$m\ddot{\varphi} = [c / 4\pi M(pl)^2] \times [(1/2)\hbar \times \Lambda(theo) - (3/2)\hbar] \quad (16)$$

In equation (16) we beautifully obtain the Planck mass M(pl) from $\sqrt{(G\hbar/c)}$! You may verify this yourself. Now let us continue working with equation (16), especially with the final term $(3/2)\hbar$. This reminds us of the quantum mechanical harmonic oscillator energy expression for the nth level:

$$E(QM) = (n + 1/2)\hbar\omega$$

Only for n = 1 do we obtain $(3/2)\hbar$:

$$E(QM) = (1 + 1/2)\hbar\omega$$

$$E(QM) = (3/2)\hbar\omega$$

$$(3/2)\hbar = E(QM)/\omega = E(QM)/2\pi\nu \quad (17)$$

In equation (17), we get the energy of the first excited state. $\omega = 2\pi\nu$ represents the transition frequency. Now substituting $(3/2)\hbar$ from equation (17) into equation (16):

$$m\ddot{\varphi} = [c / 4\pi M(pl)^2] \times [(1/2)\hbar \times \Lambda(theo) - (3/2)\hbar]$$

$$m\ddot{\varphi} = [c / 4\pi M(pl)^2] \times [(1/2)\hbar \times \Lambda(theo) - E(QM)/2\pi\nu]$$

Or more clearly:

$$\ddot{\varphi} = [c / 4\pi \times 10^{12}] \times [1 / M(pl)^2] \times (1/2)[\hbar \times \Lambda(theo) - E/\pi\nu] \quad (18)$$

We represent E(QM) simply by E. Now $c/(4\pi\times10^{12}\times M(pl)^2) = \xi$, which is a constant. And $[(1/2)\hbar\times\Lambda(theo) - E/2\pi\nu] = E(tot)$, the total energy, which is actually a conserved quantity. Later we will see how energy is conserved. Then equation (18) becomes:

$$\ddot{\varphi} = \xi \times E(tot)$$

$$(d\dot{\varphi}/dt) = \xi \times E(tot)$$

$$\int(d\dot{\varphi}/dt)dt = \xi \times E(tot)\int dt$$

$$\dot{\varphi} = \xi \times E(tot) \times t + C_1$$




©2025 Great Britain Journals Press

$$\int d\varphi = \xi \times E(tot) \times \int t\, dt + C_1 \int dt$$

$$\Delta\varphi = \xi \times E(tot) \times (1/2)\Delta t^2 + C_1\Delta t + C_2 \quad (19)$$

In equation (19), $\Delta\varphi = \varphi(f) - \varphi(i)$.

If in $\Delta t$ we put the upper time limit t(f) and lower time limit t(i) during inflation, then $\Delta t = t(f) - t(i)$. Where $t(f) = 10^{-33}$ seconds and $t(i) = 10^{-36}$ seconds. Therefore $\Delta t \approx 10^{-33}$ seconds. Thus:

$$\Delta\varphi = \xi \times E(tot) \times (1/2)\Delta t^2 + C_1\Delta t + C_2$$

$$\varphi(f) - \varphi(i) = \xi \times E(tot) \times (1/2) \times 10^{-66} + C_1 \times 10^{-33} + C_2$$

$$\Delta\varphi = \xi \times E(tot) \times (1/2) \times t(pl)^2 \times M(pl) + (10^{-33} + 1)C$$

In the above equation I set $C_1 = C_2 = C$ for mathematical convenience. $t(pl) \approx 10^{-43}$ sec, and M(pl) is about $10^{20}$ GeV. Here $(10^{-33} + 1)C \approx C$. Thus:

$$\Delta\varphi = (1/2)[c/(4\pi\times10^{12})]E(tot)\{t(pl)^2/M(pl)\} + C$$

$$\Delta\varphi = (1/2) \times \xi \times [t(pl)^2/M(pl)] \times E(tot) + C \quad (20)$$

According to equation (20), $C << 1$ and $C > 0$. Thus $C \approx 0$ may be considered, meaning extremely close to zero. As we assumed a vanishing contribution for $\varphi^{\cdot}$ under the "Sensitive-φ" condition. The "Sensitive-φ" condition allows $\varphi^{\cdot}$ to stand simultaneously near zero and non-zero. For mathematical convenience $\varphi^{\cdot}$ can be expressed in multiple ways. And quantum mechanics inherently deals with microscopic or infinitesimal corrections, matching perfectly with the Sensitive-φ condition. Therefore:

$$\Delta\varphi = (1/2) \times \xi \times [t(pl)^2/M(pl)] \times E(tot) + C$$

$$\varphi(f) - \varphi(i) = (1/2) \times \xi \times [t(pl)^2/M(pl)] \times E(tot) + C$$

$$\varphi(f) = \varphi(i) + [(1/2) \times \xi \times [t(pl)^2/M(pl)] \times E(tot) + C] \quad (21)$$

Thus from equation (21), φ(f) is slightly larger than φ(i). A minute deviation is noticeable. In quantum mechanics such minute variations cannot be ignored. In classical physics microscopic changes can often be neglected without affecting the system's macroscopic behavior. But quantum systems do not behave that way. From equation (21), E(tot) acts as the total energy term. We may call it the Hamiltonian:

E(tot) = Hamiltonian Of The System

That is:

$$H = [(1/2)\hbar\times\Lambda(theo) - E/2\pi\nu] \quad (22)$$

Now we will express H or the Hamiltonian in quantum mechanical terminology. For this we define $\hat{H}$, the Hamiltonian operator:

$$\hat{H} = [(1/2)\hbar\times\Lambda(theo) - (i\hbar\partial/\partial t) \times (1/2\pi\nu)] \quad (23)$$





©2025 Great Britain Journals Press

Here E is written in operator form $\hat{E}$:

$$\hat{E} \rightarrow i\hbar(\partial/\partial t) \tag{24}$$

Now if a state (particle state) is $|\Psi\rangle$, acting $\hat{H}$ on it gives:

$$\hat{H}|\Psi\rangle = [(1/2)\hbar\times\Lambda(theo) - (i\hbar\partial/\partial t) \times (1/2\pi v)]|\Psi\rangle$$

$$\hat{H}|\Psi\rangle = (1/2)\hbar\times\Lambda(theo)|\Psi\rangle - (1/2\pi v) \times (i\hbar\partial/\partial t)|\Psi\rangle$$

$$\hat{H}|\Psi\rangle = 0 - (1/2\pi v) \times (i\hbar\partial/\partial t)|\Psi\rangle$$

$$\hat{H}|\Psi\rangle = -[E/(2\pi v)]\,|\Psi\rangle \tag{25}$$

Here $-[E/(2\pi v)]$ represents those states possessing negative energy eigenvalues. Another thing we obtain from quantum mechanics is the entity L, whose expectation value $\langle L\rangle$ is defined:

$$\langle L\rangle = \langle\Psi|L|\Psi\rangle$$

$$(d/dt)\langle L\rangle = (d/dt)|\langle\Psi|L|\Psi\rangle|$$

$$d\langle L\rangle/dt = |\langle\Psi|L|\Psi\rangle + \langle\Psi|L|\Psi\rangle|$$

$$d\langle L\rangle/dt = (i\hbar/2\pi v)|\langle\Psi|HL|\Psi\rangle - \langle\Psi|LH|\Psi\rangle|$$

Thus:

$$d\langle L\rangle/dt = (i\hbar/2\pi v)|\langle\Psi|(HL - LH)|\Psi\rangle|$$

$$d\langle L\rangle/dt = (i\hbar/2\pi v)[H, L] \tag{26}$$

Now if L = H, since both the Lagrangian L and Hamiltonian H are conserved quantities, we may say:

$$d\langle H\rangle/dt = (i\hbar/2\pi v)[H, H]$$

$$d\langle H\rangle/dt = (i\hbar/2\pi v)[HH - HH]$$

$$d\langle H\rangle/dt = 0$$

$$\langle H\rangle = \text{Conserved} \tag{27}$$

Now let us see whether $\varphi$ and H exhibit a commutation relation:

$$[\hat{\varphi}, \hat{H}]$$

$$= (\varphi H - H\varphi)$$

$$= \varphi[(1/2)\hbar\Lambda(theo) - (E/2\pi v)] - [(1/2)\hbar\Lambda(theo) - (E/2\pi v)]\varphi$$

$$= (1/2\pi v)[-\varphi i\hbar(\partial/\partial t) + i\hbar(\partial/\partial t)\varphi]$$

Thus:




©2025 Great Britain Journals Press

$$[\hat{\varphi}, \hat{H}] = (1/2\pi v)i\hbar(\partial\varphi/\partial t)$$

$$\langle\dot{\varphi}\rangle = (2\pi v/i\hbar)[\hat{\varphi}, \hat{H}]$$

$$\langle\dot{\varphi}\rangle = (-i2\pi v/\hbar)[\hat{\varphi}, \hat{H}] \quad (28)$$

Now let us check if φ and V(φ) commute:

$$[\hat{\varphi}, \hat{V}] = (\varphi V - V\varphi)$$

$$V = (1/2)m^2\varphi^2$$

Thus:

$$[\hat{\varphi}, \hat{V}] = 1/2(m^2\varphi^3 - m^2\varphi^3)$$
$$[\hat{\varphi}, \hat{V}] = 0$$

$$\langle 0|[\hat{\varphi}, \hat{V}]|0\rangle = 0 \quad (29)$$

Now returning to equation (20):

$$\Delta\varphi = (1/2) \times \xi \times [t(pl)^2/M(pl)] \times E(tot) + C$$

If the "Sensitive-φ" condition is again implemented, we may say that:

"(1/2) × ξ × [t(pl)²/M(pl)] × E(tot)" is much smaller than 1 but slightly greater than 0, essentially almost zero. The purpose of choosing such a limit is that it allows us to track how the mathematical terms change. In quantum systems such tiny variations cannot be ignored. Because minute variations give rise to large-scale effects. We stand right at the boundary of the slow roll approximation – the "Sensitive-φ" condition. Thus Δφ ≈ C only when:

$$(1/2) \times \xi \times [t(pl)^2/M(pl)] \times E(tot) \approx 0 \quad (30)$$

$$E(tot) \approx 0$$

$$(1/2)\hbar \times \Lambda(theo) - (i\hbar\partial/\partial t) \times (1/2\pi v) \approx 0$$

$$(1/2)\hbar \times \Lambda(theo) - E(Q.M) \times (1/2\pi v) \approx 0$$

$$(1/2)\hbar \times \Lambda(theo) \approx E(Q.M) \times (1/2\pi v)$$

$$\hbar \times \Lambda(theo) \approx E(Q.M) \times (1/\pi v)$$

$$E(Q.M) \approx \pi v\hbar \times \Lambda(theo) \quad (31)$$

Here π is a number, v or transition frequency is a number, ħ is a very small positive number, and Λ(theo) is the positive cosmological constant, which itself is very small. A universe with a positive cosmological constant always expands. If there were a negative sign before Λ(theo), it would act not as a repulsive field but as an attractive one. In that case expansion would slow down or the universe would collapse back into a singularity. Dark energy field does not arise from ordinary matter particles. Instead, it determines energy states that possess negative energy eigenvalues, as seen from equation (25). That is why in the "Slow Roll Inflation" model we obtained P(φ) = –V(φ), ρ(φ) = V(φ), or ρ(φ) =





©2025 Great Britain Journals Press

$-P(\varphi)$, or $P(\varphi) = -\rho(\varphi)$, derived from $P = \omega\rho$ where $\omega = -1$ for vacuum energy or cosmological constant. In the early universe or at the beginning of inflation, the universe starts from a non-zero cosmological constant. When inflation ends and reheating begins, through thermalization dark energy or cosmological constant transforms into ordinary matter and dark matter. Despite its very small value, the effective repulsive strength of dark energy is much greater than the attractive gravity of ordinary matter or dark matter. That is why the universe is expanding.

## II. CONCLUSION

In conclusion, we may say that even vacuum carries energy. Because it contributes to a type of particle which possesses negative energy eigenvalues. And my method has beautifully quantified the dark energy particle. According to equation (23):

$$\hat{H} = [(1/2)\hbar \times \Lambda(\text{theo}) - (i\hbar\partial/\partial t) \times (1/2\pi\nu)] \quad (23)$$

$$\hat{H} = [(1/2)\hbar \times \Lambda(\text{theo}) + \{-(i\hbar\partial/\partial t) \times (1/2\pi\nu)\}]$$

$$\hat{H} = (1/2)\hbar \times \Lambda(\text{theo}) + E' \times (1/2\pi\nu)\} \quad (32)$$

It may also be written this way. Notably, in $\hat{H}$ we do not obtain any potential term. Because in the earliest epoch of the universe gravity was repulsive. Only in ordinary Newtonian or classical gravity does a potential term appear. However, in one sense $\Lambda(\text{theo})$ behaves like a negative potential of the field. The entire matter depends on how mathematical terms may be related to each other. And the force, that's i got in the equation (8), I called it Scalar force! It's probably the sakar or the sakarov definition of scalar force.

## REFERENCES


1. A. A. Starobinsky, A New Type of Isotropic Cosmological Models Without Singularity, Phys. Lett. B91 (1980) 99.
2. A. H. Guth, The Inflationary Universe: A Possible Solution to the Horizon and Flatness Problems, Phys. Rev. D23 (1981) 347.
3. A. D. Linde, A New Inflationary Universe Scenario: A Possible Solution of the Horizon, Flatness, Homogeneity, Isotropy and Primordial Monopole Problems, Phys. Lett. B108 (1982) 389.
4. A. Albrecht and P. J. Steinhardt, Cosmology for Grand Unified Theories with Radiatively Induced Symmetry Breaking, Phys. Rev. Lett. 48 (1982) 1220.
5. BICEP, KECK collaboration, Improved Constraints on Primordial Gravitational Waves using Planck, WMAP, and BICEP/Keck Observations through the 2018 Observing Season, Phys. Rev. Lett. 127 (2021) 151301 2110.00483).
6. L. Järv, K. Kannike, L. Marzola, A. Racioppi, M. Raidal, M. Rünkla et al.,





©2025 Great Britain Journals Press

Scan to know paper details and
author's profile

# Sixfold Discrete Symmetry Explains Dark Matter

*Avi Nofech*

## ABSTRACT

Using the Pauli algebra version of the Dirac equation we show the existence of its six symmetric versions whose solutions are referred to as the six sectors of fermion fields. It is shown that the sectors are distinct, by showing that if a fermion field belongs to two sectors at once then its mass must be zero. Also shown is the lack electromagnetic interaction between different sectors, since each sector has its own unique matrix coupling its fermion field to its EM field.

Altogether this predicts the ratio of dark matter to ordinary matter of 5 to 1, which is close to the observed ratio of 5.2 to 1 [3]. In order to fully justify this prediction, the sixfold discrete symmetry must first of all be extended to the electroweak sector, then to strong interactions. This article only deals with coupling of fermion fields to electromagnetic fields.

This paper essentially depends on the full equivalence of the Pauli algebra version of the Dirac equation with its standard version, which is proven in (2.1). The sixfold symmetry can be seen in the Pauli algebra version of the Dirac equation, but is harder to see in its standard version.

*Keywords:* fermion fields, discrete symmetry, mass inversion.

*Classification:* LCC Code: QC793.3.F5, QC794.6.S95, QB461

*Language:* English

Great Britain Journals Press

LJP Copyright ID: 925616
Print ISSN: 2631-8490
Online ISSN: 2631-8504

London Journal of Research in Science: Natural & Formal

Volume 25 | Issue 15 | Compilation 1.0

© 2025. Avi Nofech. This is a research/review paper, distributed under the terms of the Creative Commons Attribution-Noncom-mercial 4.0 Unported License http://creativecommons.org/licenses/by-nc/4.0/), permitting all noncommercial use, distribution, and reproduction in any medium, provided the original work is properly cited.

# Sixfold Discrete Symmetry Explains Dark Matter

Avi Nofech

## ABSTRACT

*Using the Pauli algebra version of the Dirac equation we show the existence of its six symmetric versions whose solutions are referred to as the six sectors of fermion fields. It is shown that the sectors are distinct, by showing that if a fermion field belongs to two sectors at once then its mass must be zero. Also shown is the lack electromagnetic interaction between different sectors, since each sector has its own unique matrix coupling its fermion field to its EM field.*

*Altogether this predicts the ratio of dark matter to ordinary matter of 5 to 1, which is close to the observed ratio of 5.2 to 1 [3]. In order to fully justify this prediction, the sixfold discrete symmetry must first of all be extended to the electroweak sector, then to strong interactions. This article only deals with coupling of fermion fields to electromagnetic fields.*

*This paper essentially depends on the full equivalence of the Pauli algebra version of the Dirac equation with its standard version, which is proven in (2.1). The sixfold symmetry can be seen in the Pauli algebra version of the Dirac equation, but is harder to see in its standard version.*

*Keywords:* fermion fields, discrete symmetry, mass inversion.

## I. INTRODUCTION, NOTATION, AND THE MAIN RESULTS

### *1.1 Introduction*

Dark Matter is not exotic! We show the existence of six sectors of fermion fields, of which one is our ordinary matter and five others are their symmetric twins, symmetric but not identical to ordinary matter.

The motivation for this article is the sixfold symmetry of fermion fields which is apparent in the Pauli algebra formulation [8] of the Dirac equation but is hidden in its standard four-component form.

The solutions to the six symmetric versions of the Dirac equation form what is referred to as the six sectors of fermion fields, and the solutions to six versions of Maxwell's equations form the six sectors of the electromagnetic field.

The mathematical reason for the sixfold symmetry are the six representations of the Clifford algebra $\mathrm{Cl}_{1,2}$ into the algebra of two-by-two complex matrices $M_2(\mathbb{C})$. The key to this is the table in Section 6.

The group of discrete symmetries of fermion fields are the automorphisms of the first Pauli group $G_1$, with inner automorphisms containing the charge conjugation and the mass inversion [8]. The outer automorphisms are the subgroup of order two with the parity involution, taken direct product with the permutation group on three letters. (See 9.1).



©2025 Great Britain Journals Press

We construct an operator that calculates the values of the electric and magnetic fields coupled to the fermion field out of the fermion field spinor, with all quantities taking values in the Pauli algebra of two by two complex matrices (4.1). The resulting second order wave equation has a coupling matrix which is unique for each of the six versions, obtained by applying the outer automorphisms of the Pauli algebra.

The six versions of the Dirac equation do have the same scalar equations, which raises a question, will their solutions be distinct? This question is answered positively in (7) by showing that if a field belongs to two different sectors then its mass equals zero.

Another naturally arising question is, does there exist any electromagnetic transmission between different sectors? It is answered in the negative in (4.1). For each of the six sectors, there is a different coupling matrix connecting its electromagnetic field to its fermion field, thus precluding electromagnetic signals between different sectors.

### 1.2 Notation

All quantities considered here are elements of the Pauli algebra of complex $2 \times 2$ matrices, written in the basis of Pauli matrices. Only lower indices are used and instead of upper and lower indices the change of sign of the vector component is indicated by the bar. $\sigma_0$ being identity is omitted.

$$\begin{aligned} a &= a_0 + \underline{a} = \sigma_0 a_0 + \sigma_1 a_1 + \sigma_2 a_2 + \sigma_3 a_3 \\ \overline{a} &= a_0 - \underline{a} = \sigma_0 a_0 - \sigma_1 a_1 - \sigma_2 a_2 - \sigma_3 a_3 \\ a\overline{a} &= \overline{a} a = \det a \end{aligned}$$

Any element can be written as sum of its scalar component and its vector component. The "bar" operation switches the sign of the vector component leaving the scalar component unchanged. The "star" operation is taking the Hermitian conjugate. Their composition "bar-star", in either order, is an automorphism of the Pauli algebra, similar to complex conjugation. It is an outer automorphism since it replaces the determinant of an element with its complex conjugate. The subalgebra $\mathbb{H} \in M_2(\mathbb{C})$ fixed by the bar-star automorphism is called the subalgebra of real quaternions, and their products with $i$ are called imaginary quaternions. Their sign is changed by the bar-star operation.

$$u, v \in \mathbb{H} \quad \Longleftrightarrow \quad \overline{u}^* = u \qquad \overline{(iv)}^* = -iv \qquad \overline{u + iv}^* = u - iv$$

It is shown in [8] that the bar-star automorphism is the parity symmetry.

A real quaternion $u = u_0 + \underline{u}$ has a real scalar component $u_0$ and imaginary vector component $\underline{u}$, vice versa for imaginary quaternions.

The differential, where $\partial_\alpha$ stands for $\frac{\partial}{\partial x_\alpha}$:

$$\begin{aligned} \partial &= \partial_0 + \underline{\partial} = \sigma_0 \partial_0 + \sigma_1 \partial_1 + \sigma_2 \partial_2 + \sigma_3 \partial_3 \\ \bar{\partial} &= \partial_0 - \underline{\partial} = \sigma_0 \partial_0 - \sigma_1 \partial_1 - \sigma_2 \partial_2 - \sigma_3 \partial_3 \end{aligned} \tag{1.1}$$

Their composition in either order is the d'Alembertian, multiplied by the identity matrix:

$$\partial\overline{\partial} = \overline{\partial}\partial = \Box$$


©2025 Great Britain Journals Press

The EM four-potential: $A = A_0 + \underline{A} = \sigma_0 A_0 + \sigma_1 A_1 + \sigma_2 A_2 + \sigma_3 A_3$

Inner and outer products of vector components:

$$\underline{a} \cdot \underline{b} \ := \frac{1}{2}(\underline{a}\,\underline{b} + \underline{b}\,\underline{a}) \qquad \underline{a} \wedge \underline{b} \ := \frac{1}{2}(\underline{a}\,\underline{b} - \underline{b}\,\underline{a}) \qquad \underline{a}\,\underline{b} = \underline{a} \cdot \underline{b} + \underline{a} \wedge \underline{b}$$

$$\underline{a} \cdot \underline{b} = a_1 b_1 + a_2 b_2 + a_3 b_3 \qquad \underline{a} \wedge \underline{b} = \begin{vmatrix} i\sigma_1 & i\sigma_2 & i\sigma_3 \\ a_1 & a_2 & a_3 \\ b_1 & b_2 & b_3 \end{vmatrix}$$

The electric and magnetic fields:

$$E = -\partial_0 \underline{A} - \underline{\partial} A_0 \qquad i\underline{B} = \underline{\partial} \wedge \underline{A} = \begin{vmatrix} i\sigma_1 & i\sigma_2 & i\sigma_3 \\ \partial_1 & \partial_2 & \partial_3 \\ A_1 & A_2 & A_3 \end{vmatrix}$$

The four-component spinor of the Dirac equation is written using letters rather than indices and is completed with the second column as follows:

$$\Psi = \begin{bmatrix} a \\ b \\ c \\ d \end{bmatrix} \longrightarrow \begin{bmatrix} a & b^* \\ b & -a^* \\ c & -d^* \\ d & c^* \end{bmatrix} = \begin{bmatrix} iv \\ \\ u \end{bmatrix}$$

The lower square of the two-column matrix is an element $u$ of the subalgebra of real quaternions $\mathbb{H}$ and is unchanged by the bar-star automorphism. The upper square $iv$ is a product of a real quaternion with imaginary unit $i$ and its sign is changed by the bar-star automorphism (this can be checked by direct calculation). Their sum is called the Pauli algebra spinor:

$$u = \begin{bmatrix} c & -d^* \\ \\ d & c^* \end{bmatrix} \qquad iv = \begin{bmatrix} a & b^* \\ \\ b & -a^* \end{bmatrix} \qquad \psi = u + iv \qquad \overline{\psi}^* = u - iv$$

### 1.3 The Main Results

a) Pauli algebra Dirac equation and the inhomogeneous wave equation for our sector, both with their bar-star conjugates, see Section 5.

b) The second order wave equation coupling the fermion field to EM field:

$$\left(\Box + \mathrm{m}^2 - \mathrm{q}^2 \det A\right) \ \psi(i\sigma_3) = \mathrm{q}\,(\bar{\partial}\bar{A} + A\partial)\psi$$

where $i\sigma_3$ is the coupling matrix, again specifically for our sector.

c) The six symmetric versions of all equations: they are obtained from the six different representations of the Clifford algebra $\mathrm{Cl}_{1,2}$ into the algebra of matrices $M_2(\mathbb{C})$. Each of these versions has its own coupling matrix that connects between the fermion field and the EM field.





©2025 Great Britain Journals Press

d) The group of discrete symmetries of fermion fields: they correspond to the group of automorphisms of the first Pauli group $G_1$, with inner automorphisms being the charge conjugation, the mass inversion, and their composition, and the outer automorphisms being the group of order two containing the parity involution taken direct product with the group of permutations on three letters. (see 9.1)

## II. PROOF OF EQUIVALENCE OF THE PAULI ALGEBRA VER SION TO THE STANDARD DIRAC EQUATION

**Proposition 2.1.** *The standard Dirac equation taken together with its Hermitian conjugate is equivalent to the Pauli algebra Dirac equation taken together with its bar-star image.*

*Proof.* The original Dirac equation: $(i\gamma^\mu D_\mu - \mathrm{m})\,\Psi = 0$ is multiplied by $-i$ and is rewritten in two by two blocks with separate matrices for the differentials and for the EM interaction term. The left column of the equation below are the four scalar equations of the standard Dirac equation and the right column are the equations of the Hermitian conjugate Dirac equation, though they appear in different order. The matrices $i\sigma_3$ appear because without them the right column would have the opposite sign.

$$\begin{bmatrix} \partial_0 & \underline{\partial} \\ -\underline{\partial} & -\partial_0 \end{bmatrix} \begin{bmatrix} iv \\ u \end{bmatrix} + \mathrm{q} \begin{bmatrix} A_0 & -\underline{A} \\ \underline{A} & -A_0 \end{bmatrix} \begin{bmatrix} iv \\ u \end{bmatrix} \Big[i\sigma_3\Big] + \mathrm{m} \begin{bmatrix} iv \\ u \end{bmatrix} \Big[i\sigma_3\Big] = 0 \qquad (2.1)$$

(It is useful at this point to rewrite the equation without blocks and check that the four equations in the left column are those of the Dirac equation and the four equations in the right column are of its Hermitian conjugate).

We now multiply the equation on the right by $i\sigma_3$ and rewrite it as two equations in Pauli algebra, and also switch the signs in the second equation:

$$\begin{aligned} \partial_0 iv(i\sigma_3) + \underline{\partial}\, u(i\sigma_3) - \mathrm{q}\, A_0 iv + \mathrm{q}\, \underline{A} u - \mathrm{m}\, iv = 0 \\ \partial_0 u\,(i\sigma_3) + \underline{\partial}\, iv(i\sigma_3) - \mathrm{q}\, A_0 u + \mathrm{q}\, \underline{A} iv + \mathrm{m}\; u = 0 \end{aligned}$$

Next add and subtract the two equations recalling that $\psi = u + iv$, $\overline{\psi}^* = u - iv$:

$$\begin{aligned} \partial_0 \psi\; (i\sigma_3) + \underline{\partial}\psi\; (i\sigma_3) - \mathrm{q}\, A_0 \psi + \mathrm{q}\, \underline{A}\psi + \mathrm{m}\, \overline{\psi}^* = 0 \\ \partial_0 \overline{\psi}^* (i\sigma_3) - \underline{\partial}\, \overline{\psi}^* (i\sigma_3) - \mathrm{q}\, A_0\, \overline{\psi}^* - \mathrm{q}\, \underline{A}\, \overline{\psi}^* + \mathrm{m}\, \psi = 0 \end{aligned}$$

We obtain the Pauli algebra Dirac equation and its bar-star conjugate:

$$\begin{aligned} \partial\, \psi\; (i\sigma_3) - \mathrm{q}\, \bar{A}\psi + \mathrm{m}\, \overline{\psi}^* = 0 \\ \bar{\partial}\overline{\psi}^* (i\sigma_3) - \mathrm{q}\, A \overline{\psi}^* + \mathrm{m}\, \psi = 0 \end{aligned} \qquad (2.2)$$

These two equations are transformed one into the other by the bar-star automorphism, because $\partial$ and $A$ are real. □


©2025 Great Britain Journals Press

## III. OBTAINING THE MAXWELL'S EQUATIONS FROM THE PAULI ALGEBRA DIRAC EQUATIONS

We apply the differential $\partial$ to the four-potential $A$:

$$\partial A = (\partial_0 + \underline{\partial})(A_0 + \underline{A}) = \partial_0 A_0 + \underline{\partial} \cdot \underline{A} \,| + \partial_0 \underline{A} + \underline{\partial} A_0 \,| + \underline{\partial} \wedge \underline{A} = L - \underline{E} + i\underline{B}$$

where the three summands are the scalar Lorentz sum, the electric field and the magnetic field.

Next apply the bar-star conjugate of the differential, whose composition with differential is the d'Alembertian, and that the current $J = \Box A$: (see Eq. 5.1)

$$J = \Box A = \overline{\partial}(\partial A) = (\partial_0 - \underline{\partial})(L - \underline{E} + i\underline{B}) =$$
$$= \partial_0 L - \partial_0 \underline{E} + \partial_0 i\underline{B} - \underline{\partial} L + \underline{\partial} \cdot \underline{E} + \underline{\partial} \wedge \underline{E} - i\underline{\partial} \cdot \underline{B} - i\underline{\partial} \wedge \underline{B}$$

The summands in this equation are of four different types and we rewrite the four separate sub-equations for each type:

$$\begin{aligned} \textit{real scalar} \qquad & \partial_0 L + \underline{\partial} \cdot \underline{E} = 0 \\ \textit{imaginary scalar} \qquad & \underline{\partial} \cdot i\underline{B} = 0 \\ \textit{real vector} \qquad & \underline{J} + \partial_0 \underline{E} + \underline{\partial} L + \underline{\partial} \wedge i\underline{B} = 0 \\ \textit{imaginary vector} \qquad & \partial_0 \, i\underline{B} + \underline{\partial} \wedge \underline{E} = 0 \end{aligned}$$

In order to see that these are the four Maxwell's equations we rewrite them in a more traditional order:

$$\begin{aligned} \underline{\partial} \cdot \underline{E} &= -\partial_0 L \\ \underline{\partial} \cdot i\underline{B} &= 0 \\ \underline{\partial} \wedge \underline{E} &= -\partial_0 \, i\underline{B} \\ \underline{\partial} \wedge i\underline{B} &= -\underline{J} - \partial_0 \underline{E} - \underline{\partial} L \end{aligned}$$

The Lorentz sum $L$ appears in the equations because there was no fixing of a gauge. Its time derivative is minus the charge density. The minus sign before the current in the last equation is because the wedge product introduces one more copy of $i$ and $i^2 = -1$. See also [5].

## IV. SECOND ORDER WAVE EQUATION COUPLING THE FERMION AND THE EM FIELDS

### *4.1 Reciprocal expressions for the spinor and its bar-star image*

The equations 2.2 allow to express $\overline{\psi}^*$ in terms of $\psi$ and vice versa express $\psi$ in terms of $\overline{\psi}^*$. Then combine to obtain second order equations for both:

$$\begin{aligned} \overline{\psi}^* &= -\frac{1}{\mathrm{m}} \left( \partial \, \psi \;\; (i\sigma_3) - \mathrm{q} \, \bar{A} \, \psi \right) \\ \psi &= -\frac{1}{\mathrm{m}} \left( \bar{\partial} \, \overline{\psi}^* (i\sigma_3) - \mathrm{q} \, A \, \overline{\psi}^* \right) \end{aligned}$$

London Journal of Research in Science: Natural & Formal



©2025 Great Britain Journals Press

Now plug in:

$$\begin{aligned}\psi &= \frac{1}{\mathrm{m}^2}\left(\bar{\partial}\left(\partial\psi\,(i\sigma_3)-\mathrm{q}\bar{A}\psi\right)\,(i\sigma_3)-\mathrm{q}A\left(\partial\psi\;\;(i\sigma_3)-\mathrm{q}\bar{A}\psi\right)\right)\\ \overline{\psi}^* &= \frac{1}{\mathrm{m}^2}\left(\partial\left(\bar{\partial}\overline{\psi}^*(i\sigma_3)-\mathrm{q}A\overline{\psi}^*\right)(i\sigma_3)-\mathrm{q}\bar{A}\left(\bar{\partial}\overline{\psi}^*(i\sigma_3)-\mathrm{q}A\,\overline{\psi}^*\right)\right)\end{aligned}$$

Simplify:

$$\begin{aligned}\psi &= \frac{1}{\mathrm{m}^2}\left(-\Box\psi-\;\mathrm{q}\bar{\partial}(\bar{A}\psi)(i\sigma_3)\;-\mathrm{q}A\partial\;\psi(i\sigma_3)\;+\mathrm{q}^2\det(A)\psi\right)\\ \overline{\psi}^* &= \frac{1}{\mathrm{m}^2}\left(-\Box\overline{\psi}^*-\mathrm{q}\partial(A\overline{\psi}^*)(i\sigma_3)-\mathrm{q}\bar{A}\bar{\partial}\;\overline{\psi}^*(i\sigma_3)+\mathrm{q}^2\det(A)\overline{\psi}^*\right)\end{aligned}$$

Rewriting we have:

$$\begin{aligned}\left(\Box+\mathrm{m}^2-\mathrm{q}^2\det A\right)\psi &= -\mathrm{q}\left(\bar{\partial}\bar{A}+A\partial\right)\;\;\psi(i\sigma_3)\\ \left(\Box+\mathrm{m}^2-\mathrm{q}^2\det A\right)\overline{\psi}^* &= -\mathrm{q}\left(\partial A+\bar{A}\bar{\partial}\right)\;\overline{\psi}^*(i\sigma_3)\end{aligned}$$

Multiplying on the right by $i\sigma_3$ we have:

**Proposition 4.1.** *Coupling of Fermion and EM Fields*

$$\begin{aligned}\left(\Box+\mathrm{m}^2-\mathrm{q}^2\det A\right)\psi\,(i\sigma_3) &= \mathrm{q}\left(\bar{\partial}\bar{A}+A\partial\right)\psi\\ \left(\Box+\mathrm{m}^2-\mathrm{q}^2\det A\right)\overline{\psi}^*(i\sigma_3) &= \mathrm{q}\left(\partial A+\bar{A}\bar{\partial}\right)\;\overline{\psi}^*\end{aligned}$$

Again, these two equations are transformed one into the other by the bar-star automorphism.

Taking into account the placement of brackets in 4.1, the right sides should be understood as

$$\begin{aligned}\left(\Box+\mathrm{m}^2-\mathrm{q}^2\det A\right)\psi\,(i\sigma_3) &= \mathrm{q}\bar{\partial}(\bar{A}\,\psi)+\mathrm{q}A(\partial\,\psi)\\ \left(\Box+\mathrm{m}^2-\mathrm{q}^2\det A\right)\overline{\psi}^*(i\sigma_3) &= \mathrm{q}\partial(A\overline{\psi}^*)+\mathrm{q}\bar{A}(\bar{\partial}\overline{\psi}^*)\end{aligned}\tag{4.1}$$

## V. THE PAULI ALGEBRA LAGRANGIAN

The purpose of this section is to rewrite the Lagrangian of quantum electrodynamics in Pauli algebra form. Then the Lagrangian is rewritten in terms of Clifford algebra $\mathrm{Cl}_{1,2}$. Next we use the six representations of the Clifford algebra $\mathrm{Cl}_{1,2}$ into the algebra of two by two complex matrices $M_2(\mathbb{C})$ so as to construct the six symmetric forms of the Dirac Lagrangian and of the Dirac equation.

The main diference between the standard QED Lagrangian [6], [9], [11]:

$$\mathscr{L}_{QED}=\overline{\Psi}\left(i\gamma^\mu\partial^\mu-m\right)\Psi-qA_\mu\overline{\Psi}\gamma^\mu\Psi-\tfrac{1}{4}F^{\mu\nu}F_{\mu\nu}$$

and the Pauli algebra Lagrangian used here is use of the multiplicative structure of the algebra.


©2025 Great Britain Journals Press

and the Pauli algebra Lagrangian used here is use of the multiplicative structure of the algebra.

The other difference is that unlike the usual recovering the equations of motion from the Lagrangian using the Euler-Lagrange equations, another procedure is used, namely equating to zero the formal derivatives. This results in Pauli algebra Dirac equation [8], and the inhomogeneous wave equations.

Here is the Pauli algebra version of the QED Lagrangian:

$$\begin{aligned}\mathscr{L} &= {}^{*}\partial\,\psi(i\sigma_3) - q\psi^{*}\bar{A}\,\psi + m\psi^{*}\overline{\psi}^{*} + \left(\overline{\partial A}\right)\partial A + \\ &+ {}^{-}\bar{\partial}\,\overline{\psi}^{*}(i\sigma_3) - q\overline{\psi}A\overline{\psi}^{*} + m\,\overline{\psi}\,\psi + \left(\overline{\bar{\partial}\bar{A}}\right)\bar{\partial}\bar{A}\end{aligned}$$

The Lagrangian is intentionally written in two lines because these lines are transformed one into the other by the bar-star automorphism of the Pauli algebra (see [8]).

The Lagrangian can also be written in terms of the conserved current $J$:

$$\begin{aligned}\mathscr{L} &= {}^{*}\partial\,\psi(i\sigma_3) - \frac{1}{2}(\bar{A}\,J + \bar{J}\,A) + m\psi^{*}\overline{\psi}^{*} + \bar{A}\,\Box\,A \\ &+ {}^{-}\bar{\partial}\,\overline{\psi}^{*}(i\sigma_3) - \frac{1}{2}(A\,\bar{J} + J\,\bar{A}) + m\,\overline{\psi}\,\psi + A\,\Box\,\bar{A}\end{aligned}$$

The reason for this is that $\bar{\partial}\partial A = \partial\bar{\partial}A = \Box\,A$ and also (see 5.3)

$$q\psi^{*}\bar{A}\,\psi + q\overline{\psi}A^{\,-*} = \frac{1}{2}(\bar{A}\,J + A\,\bar{J} + \bar{J}\,A + J\,\bar{A})$$

Recovering the equations of motion is done by equating to zero the formal derivatives of the Lagrangian with respect to $\psi^{*}$, $\overline{\psi}$, $\bar{A}$, $A$:

$$\frac{\partial\mathscr{L}}{\partial\psi^{*}} = 0 \qquad \frac{\partial\mathscr{L}}{\partial\overline{\psi}} = 0 \qquad \frac{\partial\mathscr{L}}{\partial\bar{A}} = 0 \qquad \frac{\partial\mathscr{L}}{\partial A} = 0$$

This results in four equations:

$$\begin{aligned}\partial\,\psi\,(i\sigma_3) - q\bar{A}\,\psi + m\overline{\psi}^{*} &= 0 \\ \bar{\partial}\,\overline{\psi}^{*}(i\sigma_3) - qA\,\overline{\psi}^{*} + m\,\psi &= 0 \\ -J + \Box\,A &= 0 \\ -\bar{J} + \Box\,\bar{A} &= 0\end{aligned} \tag{5.1}$$

The first two equations are the Pauli algebra Dirac equation [8], and the last two are the inhomogeneous wave equations [4].

The sign of the d'Alembertian used here is the opposite of the sign in [4].

The differential, the four-potential and the four-current are elements of the Pauli algebra $M_2(\mathbb{C})$ split into scalar and vector parts as follows:

$$\begin{aligned}\partial &= \partial_\mu\sigma_\mu = \partial_0 + \underline{\partial} & \bar{\partial} &= \partial_0 - \underline{\partial} \\ A &= A^\mu\sigma_\mu = A^0 + \underline{A} & \bar{A} &= A^0 - \underline{A} \\ J &= J^\mu\sigma_\mu = J^0 + \underline{J} & \bar{J} &= J^0 - \underline{J}\end{aligned}$$





©2025 Great Britain Journals Press

If $u \in \mathbb{H}$ then $u^* = \bar{u}$, $\overline{u}^* = u$. For $iv$ the opposite holds $(iv)^* = -i\bar{v}$.

For any $\boldsymbol{\psi} \in M_2(\mathbb{C})$ $\bar{\psi}\psi = \det(\boldsymbol{\psi}) I_2$

Both compositions of the differential and its bar are the d'Alembertian: $\partial\bar{\partial} = \bar{\partial}\partial = \Box$. Hence:

$$\overline{(\partial A)}\partial A = \bar{A}\bar{\partial}\partial A = \bar{A}\,\Box\, A$$
$$\overline{(\bar{\partial}\bar{A})}\bar{\partial}\bar{A} = A\partial\bar{\partial}\bar{A} = A\,\Box\,\bar{A}$$

The Lagrangian is rewritten separating the elements into their scalar and vector parts. This will be used when writing the representation independent form of the Lagrangian.

$$\begin{aligned}\mathscr{L} \;=\; & \overset{*}{\boldsymbol{\psi}}(\partial_0 + \underline{\partial})\,\boldsymbol{\psi}(i\sigma_3) + m\psi^*\overline{\boldsymbol{\psi}}^* + \overline{\boldsymbol{\psi}}\,(\partial_0 - \underline{\partial})\,\overline{\boldsymbol{\psi}}^*(i\sigma_3) + m\,\overline{\psi}\,\psi \\ & -\frac{1}{2}[(A^0 - \underline{A})\,(J^0 + \underline{J}) + (J^0 - \underline{J})\,(A^0 + \underline{A})] + (A^0 - \underline{A})\,\Box\,(A^0 + \underline{A}) \\ & -\frac{1}{2}[(A^0 + \underline{A})\,(J^0 - \underline{J}) + (J^0 + \underline{J})\,(A^0 - \underline{A})] + (A^0 + \underline{A})\,\Box\,(A^0 - \underline{A})\end{aligned}$$

Taking into account that

$$\boldsymbol{\psi}^* = \bar{u} - i\bar{v} \qquad \bar{\boldsymbol{\psi}} = \bar{u} + i\bar{v} \qquad \overline{\boldsymbol{\psi}}^* = u - iv \qquad \psi = u + iv$$

and the expressions for the current ([7], Proposition 8) which imply:

$$J^\alpha = \frac{1}{2}\,\mathrm{tr}\,(\,\overset{*}{\boldsymbol{\psi}}\sigma^\alpha\boldsymbol{\psi}\,) \qquad J^0 = q(\bar{u}u + \bar{v}v)\sigma_0 \quad \underline{J} = J^k\sigma_k = iq(\bar{u}\sigma_k v - \bar{v}\sigma_k u)\sigma_k$$

the Lagrangian is rewritten in quaternionic functions $u$ and $v$ as follows:

$$\begin{aligned}\frac{1}{2}\,\mathscr{L} = {} & (\bar{u}\partial_0 u + \bar{v}\partial_0 v)(i\sigma_3) - (\bar{u}\underline{\partial}v - \bar{v}\underline{\partial}u)\sigma_3 - \\ & -qA_0(\bar{u}u + \bar{v}v) + iqA_k(\bar{u}\sigma_k v - \bar{v}\sigma_k u) + \\ & +A_0\,\Box\,A_0 - \underline{A}\,\Box\,\underline{A} + m(\bar{u}u - \bar{v}v)\end{aligned} \tag{5.2}$$

Equating to zero the derivatives

$$\frac{\partial\mathscr{L}}{\partial\bar{u}} = 0 \qquad \frac{\partial\mathscr{L}}{\partial\bar{v}} = 0$$

results in equations

$$\partial_0 u(i\sigma_3) - \underline{\partial}v\sigma_3 - qA^0 u + iq\underline{A}v + mu = 0$$
$$\partial_0 v(i\sigma_3) + \underline{\partial}u\sigma_3 - qA^0 v - iq\underline{A}u - mv = 0$$

which are equivalent to the first two equations of 5.1, which are the Pauli algebra Dirac equations. This can be checked by multiplying the second equation by $i$ and then adding and subtracting with the first equation.

In order to have a representation-independent form of the Lagrangian, the quaternionic functions, the real $u$ and the imaginary $iv$, need to be written first in terms of sigma matrices and then in terms of generators of the Clifford algebra:




©2025 Great Britain Journals Press

$$u = \begin{bmatrix} c & -d^* \\ d & c^* \end{bmatrix} = \begin{bmatrix} c_0 + ic_1 & -d_0 + id_1 \\ d_0 + id_1 & c_0 - ic_1 \end{bmatrix} = c_0\sigma_0 + id_1\sigma_1 - id_0\sigma_2 + ic_1\sigma_3$$

$$iv = \begin{bmatrix} a & b^* \\ b & -a^* \end{bmatrix} = \begin{bmatrix} a_0 + ia_1 & b_0 - ib_1 \\ b_0 + ib_1 & -a_0 + ia_1 \end{bmatrix} = ia_1\sigma_0 + b_0\sigma_1 + b_1\sigma_2 + a_0\sigma_3$$

## 5.1 Proof that the two forms of Lagrangian are the same

**Proposition 5.1.** *The two sums forming the interaction terms in the Lagrangian are equal:*

$$q\psi^* \bar{A}\, \psi + q\overline{\psi} A\, \overline{\Psi}^* = \frac{1}{2}(\bar{A}\, J + A\, \bar{J} + \bar{J}\, A + J\, \bar{A}) \tag{5.3}$$

*Proof.* The probability current $J^\mu$ is calculated out of the real quaternionic and imaginary quaternionic components of the Pauli algebra spinor as follows:

$$J^\mu = u^*\sigma_\mu(iv) + (iv)^*\sigma_\mu u$$

(Here the components of the conserved current $J$ are understood not as numbers, but as scalar two by two matrices).

This can be checked by using the two-column completion of $\Psi$ as described in 1.2 and in [8], and then rewriting the usual formula for the probability current [11] with $2 \times 2$ blocks $iv$ and $u$.

We need to calculate separately the scalar and the vector components of the current:

$$J_0 = q[u^*u + (iv)^*(iv)]\sigma_0 \qquad \underline{J} = J_k\sigma_k = q[u^*\sigma_k(iv) + (iv)^*\sigma_k u]\sigma_k$$

(Note that both $u^*u + (iv)^*(iv)$ and $u^*\sigma_k(iv) + (iv)^*\sigma_k u$ are real scalars)

To prove 5.3 we calculate separately the left side and the right side. The spinor $= u + iv$ is decomposed as sum of a real quaternionic function $u$ and an imaginary quaternionic function $iv$. We begin with the left side:

$$\begin{aligned} &L.S. = q\psi^* \bar{A}\, \psi + q\overline{\psi} A \overline{\Psi}^* = \\ &q\,[u^* + (iv)^*](A_0 - \underline{A})\,(u + iv) + q\,[u^* - (iv)^*](A_0 + \underline{A})\,(u - iv) = \\ &= q\,(\bar{u} - i\bar{v})(A_0 - \underline{A})\,(u + iv) + q\,(\bar{u} + i\bar{v})(A_0 + \underline{A})\,(u - iv) = \\ &= 2qA_0(\bar{u}u + \bar{v}v)\sigma_0 - 2iqA_k(\bar{u}\sigma_k v - \bar{v}\sigma_k u)\sigma_k = \\ &= 2qA_0[u^*u + (iv)^*(iv)]\sigma_0 - 2qA_k[u^*\sigma_k(iv) + (iv)^*\sigma_k u]\sigma_k \end{aligned}$$

(Note that the expressions in square brackets are real scalars)

Now calculate the right side:





©2025 Great Britain Journals Press

$$
\begin{aligned}
R.S. &= \frac{1}{2}(\bar{A}\,J + A\,\bar{J} + \bar{J}\,A + J\,\bar{A}) = \\
&= \frac{1}{2}[(A_0 - \underline{A})(J_0 + \underline{J}) + (A_0 + \underline{A})(J_0 - \underline{J}) + \\
&+ (J_0 - \underline{J})(A_0 + \underline{A}) + (J_0 + \underline{J})(A_0 - \underline{A})] = \\
&= 2(A_0 J_0 - 2\underline{A} \cdot \underline{J} - 2\underline{A} \wedge \underline{J} - 2\underline{J} \wedge \underline{A}) = \\
&= 2(A_0 J_0 - 2\underline{A} \cdot \underline{J})
\end{aligned}
$$

(the last equality because the outer product is anticommutative)

Now use the expressions for the current in (5.4):

$$R.S. = 2qA_0[u^*u + (iv)^*(iv)]\sigma_0 - 2qA_k[u^*\sigma_k(iv) + (iv)^*\sigma_k u]\sigma_k \tag{5.4}$$

$L.S. = R.S.$ □

## VI. THE CLIFFORD ALGEBRA LAGRANGIAN

The Pauli algebra $M_2(\mathbb{C})$ is isomorphic to the Clifford algebra $\mathrm{Cl}_{1,2}$ so that every element can be expressed in its three generators:

$$\mathrm{e}_0^2 = 1, \qquad \mathrm{e}_1^2 = -1, \qquad \mathrm{e}_2^2 = -1 \tag{6.1}$$

The table below defines six matrix representations of $\mathrm{Cl}_{1,2}$ into $M_2(\mathbb{C})$, of which the first is chosen to be the standard one.

The automorphisms of $M_2(\mathbb{C})$ are labelled by their action on the three cyclic subgroups of order 4 of the finite quaternion group $Q_8$. These automorphisms form a group isomorphic to the group of permutations of three letters, see [2], [1].

Here the finite quaternion group is (including their opposite signs):

$$Q_8 = \{\sigma_0,\ -i\sigma_1,\ -i\sigma_2,\ -i\sigma_3\} \ \leftrightarrow\ \{1,\ \mathbf{i},\ \mathbf{j},\ \mathbf{k}\}$$

This action can be seen in the columns corresponding to the generators

$$\mathrm{e}_1,\ \mathrm{e}_2,\ \mathrm{e}_1\mathrm{e}_2$$

The subscripts $ijk$ in the following table show the isomorphism between the outer automorphisms of $Q_8$ and the group of permutations of three letters.

The morphisms between the representations are obtained by combining the inverse of one representation with another. The automorphism of $M_2(\mathbb{C})$ converting the $DE_{123}$ into $DE_{231}$ for example will be

$$\varphi_{231} \circ \varphi_{123}^{-1}$$

Here is the table for $\varphi_{ijk} : \mathrm{Cl}_{1,2} \to M_2(\mathbb{C})$:




©2025 Great Britain Journals Press

| $\varphi_{ijk}$ | $e_0$ | $e_1$ | $e_2$ | $e_1e_2$ | $e_0e_1$ | $e_0e_2$ | $e_0e_1e_2$ |
|---|---|---|---|---|---|---|---|
| $\varphi_{123}$ | $\sigma_3$ | $-i\sigma_1$ | $-i\sigma_2$ | $-i\sigma_3$ | $\sigma_2$ | $-\sigma_1$ | $-i\sigma_0$ |
| $\varphi_{231}$ | $\sigma_1$ | $-i\sigma_2$ | $-i\sigma_3$ | $-i\sigma_1$ | $\sigma_3$ | $-\sigma_2$ | $-i\sigma_0$ |
| $\varphi_{312}$ | $\sigma_2$ | $-i\sigma_3$ | $-i\sigma_1$ | $-i\sigma_2$ | $\sigma_1$ | $-\sigma_3$ | $-i\sigma_0$ |
| $\varphi_{213}$ | $\sigma_3$ | $-i\sigma_2$ | $-i\sigma_1$ | $i\sigma_3$ | $-\sigma_1$ | $\sigma_2$ | $i\sigma_0$ |
| $\varphi_{132}$ | $\sigma_2$ | $-i\sigma_1$ | $-i\sigma_3$ | $i\sigma_2$ | $-\sigma_3$ | $\sigma_1$ | $i\sigma_0$ |
| $\varphi_{321}$ | $\sigma_1$ | $-i\sigma_3$ | $-i\sigma_2$ | $i\sigma_1$ | $-\sigma_2$ | $\sigma_3$ | $i\sigma_0$ |

The action of the bar-star automorphism and of the bar and of "star" (Hermitian conjugate) anti-automorphisms on the generators of the Clifford algebra can be seen in the following table:

| operation | $e_0$ | $e_1$ | $e_2$ | $e_1e_2$ | $e_0e_1$ | $e_0e_2$ | $e_0e_1e_2$ |
|---|---|---|---|---|---|---|---|
| bar-star | -1 | 1 | 1 | 1 | -1 | -1 | -1 |
| bar | -1 | -1 | -1 | -1 | -1 | -1 | 1 |
| star | 1 | -1 | -1 | -1 | 1 | 1 | -1 |

Now use $\varphi_{123}^{-1}$ to rewrite all the vector expressions in terms of generators of the Clifford algebra, according to the first line in the table. The $\sigma_0$ being identity is omitted.

$$\begin{aligned} \underline{\partial} &= -e_0e_2\ \partial_1 + e_0e_1\ \partial_2 + e_0\ \partial_3 \\ \underline{A} &= -e_0e_2\ A^1 + e_0e_1\ A^2 + e_0\ A^3 \\ \underline{J} &= -e_0e_2\ J^1 + e_0e_1\ J^2 + e_0\ J^3 \end{aligned} \tag{6.2}$$

The other elements of the Lagrangian that depends on the representation are $i\sigma_3$ and $\sigma_3$, and according to the first line of the table, they should be replaced with $-e_1e_2$ and with $e_0$.

Now one can write the representation-independent Lagrangian, by substituting 6.2 into 5.2. In this article the substitution is done only for the case of the free Dirac equation .

If the six representations are applied to all the expressions in the Lagrangian and in the resulting equations, then the morphisms between representations will transform solutions into solutions. Both the new Pauli algebra spinors and the corresponding new equations will be different but the underlying eight equations of the Dirac equation and its Hermitian conjugate will be exactly the same.

This raises the question, will the solutions to the transformed equations be the same as before, or will they be genuinely different? This question is answered in 7.1. Only the free Dirac equation is needed there, so here is its representation-independent form:

$$(\partial_0 - e_0e_2\ \partial_1 + e_0e_1\ \partial_2 + e_0\ \partial_3)\psi + e_0e_1e_2\, m\, \overline{\psi}^*\, e_0 = 0 \tag{6.3}$$





©2025 Great Britain Journals Press

## VII. THE SIX SECTORS OF FERMION FIELDS ARE DISTINCT

The method used to show this is the mass inversion symmetry, described in [8]. For convenience this short argument is reproduced here. Given a solution $\psi$ of the free Dirac equation define $\psi' = \psi\sigma_3$. Then multiply this equation, which appears first, on the right by $\sigma_3$, and recall that $\overline{\sigma_3}^* = -\sigma_3$:

$$\partial\psi = i\,\mathrm{m}\,\overline{\psi}^*\sigma_3 \quad \partial\psi\sigma_3 = i\,\mathrm{m}\,\overline{\psi}^*\sigma_3\sigma_3 \quad \partial\psi\sigma_3 = -i\,\mathrm{m}\,\overline{(\psi\sigma_3)}^*\sigma_3 \quad \partial\psi' = -i\,\mathrm{m}\,\overline{\psi'}^*\sigma_3$$

So $\psi'$ is also a solution of the Dirac equation but with the mass of opposite sign.

**Proposition 7.1.** *Only massless spinors can be solutions to two versions of the free Dirac equation belonging to two different sectors.*

*Proof.* These are the six versions of the free Dirac equation obtained by applying the six representations to the representation-independent free Dirac equation :

$$\begin{array}{lrcl}
123 & (\partial_0 + \sigma_1\,\partial_1 + \sigma_2\,\partial_2 + \sigma_3\,\partial_3)\psi - i\,\mathrm{m}\,\overline{\psi}^*\sigma_3 & = & 0 \\
231 & (\partial_0 + \sigma_2\,\partial_1 + \sigma_3\,\partial_2 + \sigma_1\,\partial_3)\psi - i\,\mathrm{m}\,\overline{\psi}^*\sigma_2 & = & 0 \\
312 & (\partial_0 + \sigma_3\,\partial_1 + \sigma_1\,\partial_2 + \sigma_2\,\partial_3)\psi - i\,\mathrm{m}\,\overline{\psi}^*\sigma_1 & = & 0 \\
213 & (\partial_0 - \sigma_2\,\partial_1 - \sigma_1\,\partial_2 + \sigma_3\,\partial_3)\psi + i\,\mathrm{m}\,\overline{\psi}^*\sigma_3 & = & 0 \\
132 & (\partial_0 - \sigma_1\,\partial_1 - \sigma_3\,\partial_2 + \sigma_2\,\partial_3)\psi + i\,\mathrm{m}\,\overline{\psi}^*\sigma_1 & = & 0 \\
321 & (\partial_0 - \sigma_3\,\partial_1 - \sigma_2\,\partial_2 + \sigma_1\,\partial_3)\psi + i\,\mathrm{m}\,\overline{\psi}^*\sigma_2 & = & 0
\end{array} \tag{7.1}$$

Suppose that the spinor is a solution of two different equations, with the same mass. We can always use the morphisms between representation to make the first of two equations the top line 123. Now let the second equation be any other except 213 (this case will be dealt with separately). For example suppose the second equation is 231. Multiply both equations on the right by $\sigma_3$:

$$\begin{array}{lrcl}
123 & (\partial_0 + \sigma_1\,\partial_1 + \sigma_2\,\partial_2 + \sigma_3\,\partial_3)\psi' + i\,\mathrm{m}\,\overline{\psi'}^*\sigma_3 & = & 0 \\
231 & (\partial_0 + \sigma_2\,\partial_1 + \sigma_3\,\partial_2 + \sigma_1\,\partial_3)\psi' - i\,\mathrm{m}\,\overline{\psi'}^*\sigma_2 & = & 0
\end{array} \tag{7.2}$$

So $\psi'$ is a solution for the first equation with mass $-\,\mathrm{m}$ and for the second with mass $\mathrm{m}$, which is only possible if the mass is zero. This argument applies to all lines except 213 where we do not have the anticommutation.

For the lines 123 and 213 suppose that $\mathrm{m} \neq 0$ and consider also their bar-star equations:

$$\begin{array}{lrcl}
(\partial_0 + \sigma_1\,\partial_1 + \sigma_2\,\partial_2 + \sigma_3\,\partial_3)\psi - i\,\mathrm{m}\,\overline{\psi}^*\sigma_3 & = & 0 \\
(\partial_0 - \sigma_2\,\partial_1 - \sigma_1\,\partial_2 + \sigma_3\,\partial_3)\psi + i\,\mathrm{m}\,\overline{\psi}^*\sigma_3 & = & 0 \\
(\partial_0 - \sigma_1\,\partial_1 - \sigma_2\,\partial_2 - \sigma_3\,\partial_3)\overline{\psi}^* - i\,\mathrm{m}\,\psi\sigma_3 & = & 0 \\
(\partial_0 + \sigma_2\,\partial_1 + \sigma_1\,\partial_2 - \sigma_3\,\partial_3)\overline{\psi}^* + i\,\mathrm{m}\,\psi\sigma_3 & = & 0
\end{array} \tag{7.3}$$

Subtracting the first two lines and the last two lines we get

$$\frac{1}{2}(\sigma_1 + \sigma_2)(\partial_1 + \partial_2)\ \psi = i\,\mathrm{m}\,\overline{\psi}^*\sigma_3 \quad \frac{1}{2}(\sigma_1 + \sigma_2)(\partial_1 + \partial_2)\,\overline{\psi}^* = -i\,\mathrm{m}\,\psi\sigma_3$$


©2025 Great Britain Journals Press

Combining we get $\frac{1}{2\,\mathrm{m}^2}(\partial_1+\partial_2)^2\psi = \psi$ and with a change of coordinates we have an ODE

$$\frac{1}{2\,\mathrm{m}^2}\frac{\partial^2\psi}{\partial s^2} - \psi = 0$$

with real roots of its characteristic equation. So $\psi$ is an exponential function and this is incompatible with it being normalizable. □

## VIII. THE LACK OF ELECTROMAGNETIC INTERACTION BETWEEN DIFFERENT SECTORS

We consider the six symmetric versions of the equation (4.1) that links the fermion field to the electromagnetic field. In the version labeled by the permutation 123 the linking matrix is $i\sigma_3$. A look at the fourth column of the table (6) shows that the representation independent expression is $-e_1e_2$. Its values under the six representations are all different, showing a specific coupling within each sector.

There are also the six symmetric versions of Maxwell's equations, see 3. The operator $\underline{\partial}$ which equals $\sigma_1\partial_1+\sigma_2\partial_2+\sigma_3\partial_3$ under the representation $\varphi_{123}$ changes under the other representations according to the table 6. This produces six symmetric, but non-identical copies of Maxwell's equations.

## IX. THE GROUP OF DISCRETE SYMMETRIES

**Proposition 9.1.** *The group of discrete symmetries of fermion fields is the group of automorphisms of the first Pauli group $G_1$ where the abelian normal subgroup of inner automorphisms consists of identity, the charge conjugation symmetry $C$, the mass inversion symmetry $M$ and their composition. The group of outer automorphisms is a direct product of the group of order two generated by the parity symmetry, which is the bar-star automorphism, and the group of permutations on three letters, generated by permuting the three spatial derivates with the three sigma matrices.*

*Proof.* The proof consists of identifying the discrete symmetries with elements of the automorphism group $Aut(G_1)$.

The inner automorphisms of the first Pauli group $G_1$ are the conjugations by $\sigma_1$ which is the charge conjugation symmetry $C$, by $\sigma_3$ which is the mass inversion symmetry $M$, and by their product $i\sigma_2$, which is $CM = MC$.

(This appears in [8], except it appears as right multiplication by the sigma matrix rather than conjugation as here).

Rewriting the short exact sequence

$$1 \longrightarrow \mathrm{Inn}\, G_1 \longrightarrow \mathrm{Aut}\, G_1 \longrightarrow \mathrm{Out}\, G_1 \longrightarrow 1$$

we have

$$1 \longrightarrow C_2 \times C_2 \longrightarrow \mathrm{Aut}G_1 \longrightarrow C_2 \times S_3 \longrightarrow 1$$

where in the outer automorphisms the cyclic group of order two is generated by the parity transformation "bar-star" and the group of permutations permutes between spatial derivatives and the three sigma matrices.





©2025 Great Britain Journals Press

The parity transformation inverts the signs of the three spatial derivatives and the three components of the vector potential. Recalling that there are two versions of the Pauli algebra Dirac equation related by the bar-star automorphism, this transformation essentially replaces the spinor with its bar-star image $\overline{\psi}^*$ and vice versa. Since the choice between them is arbitrary, there are only six sectors of fermion fields and not twelve. The group of automorphisms of $G_1$ is described in [10]. □

## X. CONCLUSIONS AND OPEN QUESTIONS

For the six-fold discrete symmetry to be a candidate to explain dark matter, two issues need to be addressed: first, show that the six sectors of free fermion fields are genuinely distinct from each other; and second, show the absence of electro magnetic interaction between different sectors. The first issue is addressed in (7.1). The second follows from the unique matrix coupling the fermion field to the EM field in (4.1).

What remains is the important caveat, that the six-fold symmetry must be extended to weak and strong interactions to be a reasonable explanation. This is not addressed in the present article.

According to [3] the universe consists of approximately 5% ordinary baryonic matter, ~ 26% dark matter, and ~ 61% dark energy. This gives the ratio of dark matter to ordinary matter of 5.2 : 1 which is close to 5 : 1, as predicted by the six-fold symmetry.

## REFERENCES


1. J. F. Adams. *Lectures on exceptional Lie groups*. The University of Chicago Press, 1996.
2. J. F. Adams. "Spin(8), triality, $F_4$ and all that". In: *Superspace and Su pergravity*. Cambridge University Press, 1981, pp. 435–445.
3. Katherine Freese. "Status of Dark Matter in the Universe". In: *Interna tional Journal of Modern Physics D* 26.06 (2017). Proceedings, 14th Mar cel Grossmann Meeting on Recent Developments in Theoretical and Ex perimental General Relativity, Astrophysics, and Relativistic Field Theo ries (MG14) (In 4 Volumes): Rome, Italy, July 12-18, 2015, pp. 325–355. url: https://arxiv.org/abs/1701.01840.
4. David J Griffiths. *Introduction to Electrodynamics, 4th edition*. Cambridge University Press, 2017.
5. Mingjie Li and S A R Horseley. "The electronic and electromagnetic Dirac equations". In: *New Journal of Physics* 26. February (2024).
6. Stephen P. Martin and James D. Wells. *Elementary Particles and Their Interactions*. Graduate Texts in Physics. Springer Nature Switzerland AG, 2022.
7. Avraham Nofech. "Biquaternionic Dirac equation predicts zero mass for Majorana fermions". In: *Symmetry* 12.7 (2020). url: https://doi.org/ 10.3390/sym12071144.
8. Avraham Nofech. "Construction of Discrete Symmetries Using the Pauli Algebra Form of the Dirac Equation". In: *Phys. Sci. Forum* 7(1).41 (2023). Proceedings of The 2nd Electronic Conference on Universe. url: https://doi.org/10.3390/ ECU2023-14054.





©2025 Great Britain Journals Press

9. Michael E. Peskin and Daniel V. Schroeder. *An Introduction to Quantum Field Theory*. Addison-Wesley Publishing Company, 1995.
10. Michel Planat and Maurice Kibler. *Unitary reflection groups for quantum fault tolerance*. hal-00305181v1. IPNL - Institut de Physique Nucleaire de Lyon, pp. 1–21.
11. Mark Thomson. *Modern Particle Physics*. Cambridge University Press, 2013.

*Declarations*

Funding This research received no external funding. Conflicts of Interest The authors declare no conflict of interest.





©2025 Great Britain Journals Press

*This page is intentionally left blank*


©2025 Great Britain Journals Press

Scan to know paper details and
author's profile

# A Paper "On the Quantum-Mechanics of De-Sitter Space and the Aspects of Holography"

*Najmuj Sahadat Sarkar*

## ABSTRACT

The main idea I want to discuss is the possibility that quantum-mechanical de Sitter space admits a holographic description. In spirit, such a description would be a boundary-like quantum system that makes no explicit reference to gravity, yet somehow encodes the physics of the bulk. Why focus on de Sitter space? Because de Sitter space is the "elephant in the room": enormously large, highly symmetric, cosmologically relevant, and almost certainly closely related to the universe we inhabit. But unlike Anti–de Sitter space, de Sitter space has no natural boundary, which makes holography in this setting significantly more challenging. Despite this difficulty, researchers have explored many different perspectives. Discussions about de Sitter holography often resemble the story of the "Blind Men and the Elephant," where each observer touches a different part and reaches a different conclusion. Some approaches emphasize dS/CFT, others TT deformations, the swampland program, dS/dS duality, or matrix-theory–like constructions. None of these perspectives is clearly wrong, but none gives a complete picture. In this paper I present a set of "fragmentary circumstantial evidence" suggesting that certain aspects of de Sitter space may be described by a type of matrix theory. This idea was originally proposed by several theorists; here I revisit their arguments and add some additional clues.The framework I adopt is static-patch holography. A static patch is the region seen by an observer located at its center, which I call the "pode." By symmetry, there is another static patch on the opposite side of the space, whose center I call the "anti-pode."

*Keywords:* de-sitter, space, holography, fluctuations, bsff, matrices, matrix-theory, quantum, mechanics, cosmic, black hole, horizon.

*Classification:* LCC Code: QB500.268, QC173.6, QC174.12

*Language:* English

Great Britain Journals Press

LJP Copyright ID: 925617
Print ISSN: 2631-8490
Online ISSN: 2631-8504

London Journal of Research in Science: Natural & Formal

Volume 25 | Issue 15 | Compilation 1.0

© 2025. Najmuj Sahadat Sarkar. This is a research/review paper, distributed under the terms of the Creative Commons Attribution-Noncom-mercial 4.0 Unported License http://creativecommons.org/licenses/by-nc/4.0/), permitting all noncommercial use, distribution, and reproduction in any medium, provided the original work is properly cited.

# A Paper "On the Quantum-Mechanics of De-Sitter Space and the Aspects of Holography"

Najmuj Sahadat Sarkar

## ABSTRACT

*The main idea I want to discuss is the possibility that quantum-mechanical de Sitter space admits a holographic description. In spirit, such a description would be a boundary-like quantum system that makes no explicit reference to gravity, yet somehow encodes the physics of the bulk. Why focus on de Sitter space? Because de Sitter space is the "elephant in the room": enormously large, highly symmetric, cosmologically relevant, and almost certainly closely related to the universe we inhabit. But unlike Anti–de Sitter space, de Sitter space has no natural boundary, which makes holography in this setting significantly more challenging. Despite this difficulty, researchers have explored many different perspectives. Discussions about de Sitter holography often resemble the story of the "Blind Men and the Elephant," where each observer touches a different part and reaches a different conclusion. Some approaches emphasize dS/CFT, others TT̄ deformations, the swampland program, dS/dS duality, or matrix-theory–like constructions. None of these perspectives is clearly wrong, but none gives a complete picture. In this paper I present a set of "fragmentary circumstantial evidence" suggesting that certain aspects of de Sitter space may be described by a type of matrix theory. This idea was originally proposed by several theorists; here I revisit their arguments and add some additional clues.The framework I adopt is static-patch holography. A static patch is the region seen by an observer located at its center, which I call the "pode." By symmetry, there is another static patch on the opposite side of the space, whose center I call the "anti-pode." At time t = 0, spatial slices of de Sitter space resemble a sphere, with the pode at one end, the anti-pode at the other, and the cosmological horizon in the middle. At other times, one can naturally identify two horizons—one from each static patch.The basic hypothesis is that all physics inside a single static patch can be described by a holographic theory that is essentially quantum mechanics without gravity. De Sitter space behaves as a thermal system with temperature proportional to the inverse of the de Sitter radius, meaning larger de Sitter spaces are colder.The horizon carries an entropy proportional to its area. Defining this thermodynamics already assumes that the static patch is described by a unitary quantum system with a Hilbert space, a Hamiltonian, and a set of symmetry generators that form the algebra of de Sitter space. In AdS, holographic degrees of freedom live at the asymptotic boundary. De Sitter space has no such boundary, and the static patch itself has none either. One might try to place the holographic degrees of freedom near the pode or anti-pode, but this fails because a small surface near the pode does not have enough area to encode the entire static patch. The only viable location is the stretched horizon.Therefore the holographic degrees of freedom must correspond to disturbances of the horizon itself. Operators that create excitations near the pode are complicated from the holographic viewpoint, while simple operators correspond to local changes of the horizon. This parallels what happens in AdS: excitations far from the holographic degrees of freedom appear as complex operators.In a thermal de Sitter background, rare Boltzmann fluctuations can move enough degrees of freedom from the horizon to the region near the pode, assembling macroscopic objects such as black holes. Such a configuration can be described by the Schwarzschild–de Sitter geometry, which contains two horizons: a small black hole horizon and a larger cosmological horizon. For sufficiently small black holes, the spacetime contains two identical black holes—one near the pode and one near the anti-pode.The spatial slice at t = 0 is a sphere with*

London Journal of Research in Science: Natural & Formal

©2025 Great Britain Journals Press

*two small black hole horizons near the poles and the cosmological horizon at the equator.Assuming this configuration arises as a fluctuation, its probability is determined by the difference between the entropy of pure de Sitter space and the entropy of the configuration containing the black holes. The probability is exponentially suppressed, behaving like the exponential of minus the entropy difference. For small black holes, this entropy difference is proportional to the product of the de Sitter radius and the black hole mass, making such fluctuations extremely rare.This behavior is precisely what one expects from a finite quantum system with a horizon, and it strengthens the idea that the holographic description of the static patch may resemble a matrix-theory-type construction.*

*Keywords:* de-sitter, space, holography, fluctuations, bsff, matrices, matrix-theory, quantum, mechanics, cosmic, black hole, horizon.

*Author:* Mahishadal Raj College, Physics Department, West Bengal, India.



## I. INTRODUCTION/CALCULATION:

The primary aspect of quantum mechanical de-sitter space that i talking about there is a holographic theory of the de-sitter space. In original sense, some kind of boundary theory based on conventional quantum mechanics which itself make's no explicit reference of gravity but which encodes the bulk the rest of space with in the boundary, in a mysterious way which is not fully understandable! But the question we ask, why we work with de-sitter space? I think, de-sitter space is the big elephant in the room! It's a elephant, because it's big! But de-sitter space is not only big but symmetrically big! And also it's important! We may lived very similar to the de-sitter space! Some time's, we don't see the elephant in the room; perhaps it's just too big. But also sometimes, just because of our fear we pretended the elephant is not there. I think it's a good reason. But the main reason atleast from the point of view of peoples, who doing certain kind of physics, last 15 or 20 years, we call it holographic physics. So the main reason is that de-sitter space has no boundary. It has not any natural boundary to anchor the holographic degrees of freedom to the boundary. So that makes the de-sitter space little bit of complicated. That does not mean that no body does not thinking about de sitter space! When we thinking all the things and read about de sitter space, another elephant analogy come to our mind. "The Elephant And The Blind Man" –analogy! Five blind man come close to the elephant and touch its different body parts. Just try to guessing what actually it is! And they all guessing wrong. Someone touch it's tail and say it's a rope! Someone touch its pointy horns or teeth and think it's a sword!

But de-sitter conversation with me or with my physics friend, like that it's dS/cFT, or its TT, it's a swamplands, or its just dS/dS, or probably just a Matrix-theory! See, I don't say any of this is just wrong! But i have the feeling that; if we want to saw the big picture, we would use different word's! So what i gonna present today: Some "admittedly fragmentary circumstantial evidence", that de sitter space or some aspects of the de-sitter space is describe by a kind of matrix-theory. The kind of matrix-theory I'm talking about according to my knowledge: "first proposed by a group of theorists"! They proposed some "fragmentary circumstantial evidence", and i will show some more of it in this paper. And then come-up on some other aspects of the de-sitter space! It's began to the idea of "Static Patch"! So the whole frame work, that i am going to discussing is the "Static Patch Holography" or "SPH"! The Static patch of the de-sitter space is the portion we seen from an observer at the center of that Static patch. I will like to called the center of that static patch "The Pode", and this static patch come-up with pair's, at the opposite end of the Static patch called

"Anti-Pode"! So I called to Static patches, and pick one which is shot of "gauges choice", and then there is a natural opposing static patch on the other side of de-sitter space which i named "Anti pode"! And if we take a mid slice at the de-sitter space, that what you see at the left side a penrose diagram of de-sitter space. But on the right hand side there is an embedding diagram, through at time t=0, and


©2025 Great Britain Journals Press

what you can see a metric sphere! The pode at one end, the anti-pode at other end. And the horizon right middle here (fig:a)! If you don't want to slice it at t=0; but some later time or before time then you have naturally two horizon! One associated with left static patch, and one associated with right static patch! So i draw them slightly separated (fig: a)! So the basic hypothesis is that all the physics inside of the Static patch can be described by the "Holographic theory". Again the holographic theory, mean the quantum mechanics especially the different version of quantum mechanics, which does not contain gravity! Here is the metric of the de-sitter space:

$$ds^2=-f(r)dt^2+\{dr^2/f(r)\}\, r^2d\Omega^2$$

$$f(r)=(1-r^2/R^2)$$

In this paper, i consider all the physics in 4d; not any higher number of dimension. r: the schwarzschild radius of black hole! And R: is the radius of the de-sitter space. De-sitter space has thermodynamics! And it's natural the thermodynamics of the Static patch has a temperature T, which is equal to $1/2\pi R$. The bigger the space the colder it is! And it has some entropy which i called $S_0$: it's the starting basic entropy of the de-sitter space it-self! No perturbation in de-sitter space, just the static de-sitter space! And:

$$S_0=(\pi/G)R^2$$

$R^2$: The area of the horizon! But here are some hidden assumption! In order to defining the entropy or the temperature we make a huge assumption! Entropy is the part of statistical mechanics, basically quantum statistics! And to defining it we assume to make some assumptions. First of all unitary "quantum mechanics"! There are another kind of entropy that we usually don't use in general! So unitary quantum mechanics, in our case is the static patch! Or equivalently says, "A Hilbert Space Of States"! It's possible to count the number of states! There is a Hamiltonian and a notion of energy! And Important to distinguishing whether we really have the de-sitter space or rather than some other object! If we do quantum mechanics and look at the space, may be it describe a black hole, may be it describe something else! And i think, the important thing is the Symmetry of the de-sitter space! But in this paper, i don't want to describe about the Symmetry of de-sitter space! But it's very important the hamiltonian and the other generators of symmetry are that they close in a algebra O(4,1): which is the Symmetry of de-sitter space! Let's now ask: where the holographic degrees of freedom resides! In the context of AdS they reside at the boundary of AdS! I mean the asymptotic cold boundary of "Anti de-sitter space" (AdS)! But de-sitter space has no boundary! The Static patch does not have any boundary! you most likely know that "the boundary of the static patch is it's horizon"! In the Penrose diagram of de-sitter space you might think the degrees of freedom reside at the boundary of pode and anti-pode! But that's doesn't work very well! Because it has a connection with covariant entropy bound! Means, that the region around the pode, if i draw a surface around the pode here (very close to thevpode), then it's area will be very small! So the number of degress of freedom is sufficient to describe what inside the pode! But not the rest of the Static patch! So if you consider the entire static patch (fig: b), then the degrees of freedom or dof reside at horizon or symmetric horizon of de-sitter space! Now let me come to another question very briefly! I want to presume that the holographic degrees of freedom are some Q-bits, or they might be Matrix degrees of freedom, but I'm going to assume they are more simpler than that! So what are the simple degrees of freedom? If the holographic degrees of freedom reside at the stretched horizon, they have nothing to do any boundary, they don't have to do directly degrees of freedom near the pode! They have to do degrees of freedom or dof near the horizon! So thats not like to be the quasi normal modes! I mean the quasi normal modes of oscillation of the horizon! And also not the operators, which create simple disturbances near the pode! In AdS things are far from the holographic dof where they located! Those thing's tends to be complex!





©2025 Great Britain Journals Press

But things that are near the dof tends to be simple! So i would expect the dof associated with throwing something in from the pode, or the center of de-sitter space are corresponds to complex operators, and the simple operators have more to do with the disturbances of the horizon itself (fig:c)! So now I'm gonna do in this paper: "The Evidence That The Dof Of Holographic Description For De-sitter Matrix Theory"! The dof (degrees of freedom) or Holographic dof of particular kind! Means a particular way to describing What's in space??? So now, what we gonna talk about the boltzmann-fluctuation! Boltzmann fluctuations in thermal equilibrium are large scale fluctuations, crazt things, have normal freque fluctuations, for example all the gases in the room, suddenly accumulated in one corner! So they are very very improbable! Here is an example: suppose we consider a de-sitter space, there are some degrees of freedom near the horizon! But then a crazy fluctuation happen and all the degrees of freedom near the horizon move and replace near the pode and anti-pode (fig: d)! There are enough degrees of freedom, so that they can form a macroscopic object! That is extremely improbable in the thermal equilibrium of de-sitter space! Imagine our de-sitter space will have in thermal equilibrium long long in future! But then a fluctuation occurs and a macroscopic object form near the pode and anti-pode! This is highly improbable, but this is possible, as any thing can possible in our de-sitter approximation, in thermal equilibrium!

*So the only question is what is the probability?*

So, let's talk about such fluctuations in little bit technical! Firstly take the fluctuations, so that they can form macroscopic object such as black hole, near the pode! The "de-sitter schwarzschild Metric" looks same as de-sitter metric, except that for black hole, there is a extra-term! "De-sitter schwarzschild Metric" is given by:

$$f(r)=1-(r^2/R^2)-(2MG/r)$$

So, now if we do create a black hole near the pode, there will be two horizon! If we solve that equation:

$$f(r)=0$$

One is cosmic horizon, and the other horizon will be the horizon of black hole! From f(r)=0, we find that there are two positive solutions, and one negative which is unphysical! We come up on this thing later! So let's concentrate on small black holes (fig: e)! Small black holes are the black holes, which are much smaller than the de-sitter radius, or equivalently which entropy much smaller than the de-sitter entropy! Here is the penrose diagram of de-sitter schwarzschild radius (fig: e)! There are two horizons; ($r_+$) the larger horizon, that's the cosmic horizon! Behind the $r_+$ the space is exponentially expand! The other horizon is the black hole horizon ($r_-$), which collapses to the singularity, and the space is periodic! So that you can identify the left dotted line with the right dotted line! It's actually two black hole; one is on pode side and another one is on Anti-pode side! And the spatial geometry at t=0, what it would look like???

Here is the (fig: f) good-all sphere! At the middle, here is the cosmic $r_+$ horizon! But near the pode and anti-pode there is a second horizon! The pode side horizon is same as the horizon at anti-pode side! So, it's periodic in nature! So, that's the geometry of schwarzschild de-sitter (fig: f)! Now i want to think the schwarzschild de-sitter is just a result of a fluctuation which can happen primary de-sitter space! And what is the probability for??? The probability for it:

$$P=e^{(-\Delta S)}$$

$$\Delta S=S_0-S$$


©2025 Great Britain Journals Press

$S_0$: Is the starting entropy of de-sitter space at thermal equilibrium! S: The Entropy not only for one black hole, but the whole thing subject to the condition that the two black holes are present! On other words, the conditional entropy that the two black holes are present + everything else! And the difference of this two entropy is small if the black holes are small! But what ever the entropy difference is; the probability for formation of this kind of fluctuation is e^−(ΔS)! So:

$$\Delta S=(\pi/G)\times[R^2-(r^2_{+}+ r^2_{-})]$$

$r^2_{+}$: Thats the entropy associated with the cosmic horizon, and $r^2_{-}$: is the entropy associated with the black hole! So the difference $S_0-S$ is exactly the expression: ΔS!

If there is no black hole, then $r_{+}$ is just capital "R"! And the entropy difference would be ΔS=0! And then the probability is just 1, but logically there would be no probability such as 1 or close to 1! Now, if you plug-in, what the value of $r_{+}$ and $r_{-}$ you get ΔS=2πRM! You know it's not hard to do; and very straight forward! R: The size of de-sitter space, and M: is the mass of the black hole! So:

$$\Delta S=2\pi RM \text{ :LEADING IN "M"}$$

2πRM: This quantity here also happen to be boltzmann weight for the production of black hole! And 2πR~1/T (one over the temperature)!

Or, $2\pi R=\beta=T^{-1}$; M is also the energy of the black hole; 2πR: is the boltzmann weight and it goes to the exponent and gives you the probability for such a fluctuation to be happen! There is another form which i find very interesting! It has higher dimensional generalization! Big "R" is the square root of entropy in de-sitter space! Big "M" is proportional to the entropy of black hole! So if you put this together and go through the calculation you may find:

$$\Delta S=\sqrt{(S_0 \bullet s)} \text{ : LEADING IN s!}$$

Keep this formula in mind, because there is a hint (or, a clue=???) about the structure of degrees of freedom! That clue first discussed in 2006, and later by L.susskind (2011)! So the clue or the result of the clue inside the matrix-theory! I mean, the matrix structure for the degrees of freedom in de sitter space (fig: g)! Let's start with matrix with big square arrays, N×N of them (fig: g)!Roughly speaking matrices show-up in the theory of "Do-brane"! You can think of this Do-brane ; but i think you don't habe to! The diagonal elements represent the position of Do-brane! But for the moment they are matrices, and I'm going to assume in thermal equilibrium; all of this matrix elements are the degrees of freedom! So there are $N^2$=degrees of freedom! And in thermal equilibrium each of one carry some entropy! And the total entropy is proportional to the number of Degrees of freedom! Means, $S_0=\sigma N^2$! σ: represent entropy per little degree of freedom! If you ask me How you calculate? Actually i don't know, how to calculate! So just called it σ! Now how can we describe a system in matrix theory? I am coming-up on the original "BFSS"–matrix theory(fig: h)! But in this paper i don't describe the "BFSS"–matrix theory more detail, it's just an inspiration as you might think! How we would think about some system which divided into two subsystem! In this case, the two divided sub-system are the "Horizon degrees of freedom", and "The horizon that separated the two black holes"(see fig: h)! One who studied matrix theory give you a quick answer! One block of the matrix associated with one-degrees of freedom, and the other block associated with the other degrees of freedom! The off-diagonal elements are unexcited! Classically Say's, this off-diagonal matrix elements are set to be zero! The small subsystem in "BFSS"–matrix have m×m degrees of freedom, and the big subsystem in "BFSS"–matrix have $(N-m)^2$ degrees of freedom! So:





©2025 Great Britain Journals Press

$$S=\sigma\bullet(N-m)^2 \text{ :Cosmic Horizon Entropy!}$$

$$s=\sigma\bullet m^2 \text{ :Black Hole Horizon Entropy!}$$

After thermal fluctuations, the entropy of cosmic horizon decreases, that means there are few degrees of freedom in thermal equilibrium! So, the condition entropy $S<<S_0$! $S_0$ is the original entropy in de-sitter space! And the black hole entropy $s=\sigma\bullet m^2$! So, now what about $\Delta S$???

$$\Delta S=S_0-S-s$$

$$\Delta S=\sigma\bullet N^2-\sigma\bullet(N-m)^2-\sigma\bullet m^2$$

$$\Delta S=2\sigma(m\bullet N)$$

$\Delta S$: is simply the number of constraints $\times\sigma$! If we looked at the "BFSS"–matrix structure ; we may find out that (fig: h) there are two off-diagonal matrix structure, where off-diagonal elements are set to zero! So that the entropy difference by constraining the system in that way!

$$\Delta S=2\sqrt{(S\bullet s)}$$

The big "S" proportional to$\sim(N-m)^2$ or $(N-m)\sim\sqrt{S}$! And small "s" is proportional to$\sim m^2$, or $m\sim\sqrt{s}$! And the whole result is $2\sqrt{(S\bullet s)}$! $\Delta S=2\sqrt{(S\bullet s)}$ is exactly the same formula that i derived-out starting with the de-sitter schwarzschild black hole! And calculating the entropy difference! It's lil, bit of surprise that they two match together despite the factor of 2! The entropy is the product of two subsystem entropy is not a normal thing! It's not the thing that we see everyday! Because the general relativistic calculation of $\Delta S$, and Matrix calculation of $\Delta S$ is just equal to each other! Let me give an example which does not give that type of formula! Here is the "Toy-Model" ( see fig: i)! (fig: i) You have a potential which has a "peak" at the center, a "up side down" harmonic ossicilator, and all of the particles or most of the particles sit at the bottom of (minimum) the potential! And give the system a large entropy! In thermal equilibrium the particles typically sit at the bottom of the well! But there is a tiny probability that the particles or some particle sit top of the potential, due to thermal fluctuations! I won't go through the calculations, it's elementary just elementary statistical mechanics!

$$S_0=N\bullet\log V$$

$$S=(N-m)\bullet\log V+m\bullet\log v$$

$$\Delta S=m\bullet\log(V/v)=2m\bullet\log s/S_0$$

$$\Delta S\sim m\bullet\log(m/N)$$

$$\Delta S\sim s\bullet\log(s/S)$$

So, the $\Delta S$ or differential entropy, proportional to the entropy of small subsystem (where few degrees are sit on) times logarithm of small subsystem entropy "s" :minus(–): logarithm of large subsystem entropy "S"! And it does not like anything like the product:

$$\Delta S=2\sigma N\bullet m\sim\sqrt{(s\bullet S)}$$

There are many of the mode you can construct and none of them looked like$\sim\sqrt{(s\bullet S)}\rightarrow$this! Except the matrix construction! So this type of formula $\Delta S\sim\sqrt{(s\bullet S)}$ intimately connected with the constraints $\Delta S$ formula connected with little "m" and "(N–m)"! So, $\Delta S\approx\sqrt{(s\bullet S)}$ show's a very interesting correspondence between "Matrix-theory"; "Statistical Mechanics"; and "Schwarzschild de-sitter"! Now i come-up on a very difficult problem; not too much difficult!!! But giving up the assumptions, of small black holes, we study various kind of black holes of entire mass range; from smaller possible black holes, to large mass black holes in de-sitter space!




©2025 Great Britain Journals Press

## II. FOR LARGE BLACK HOLES

$$(s/S)\sim 1$$

Means that the black hole at the same order as cosmic horizon! So that's why, s=S, equal to each other!

$$f(r)=1-(r^2/R^2)-(2MG/r)$$

$$rf(r)=r-(r^3/R^2)-2MG=0$$

Suppose i want to find out where The horizon are??? What is the value of r, R??? Then i have to set f(r)=0, but that's nasty things nasty because there is a (−2MG/r) in f(r) expression!

$$rf(r)=0$$

Now, you have a polynomial cubic equation! This cubic equation has three roots! The cubic that i drawn in deep-black (see fig: j)!

So (according to fig: j) one root is −ve, and it has no physical meaning! But other two roots ($r_-$) and ($r_+$) are positive. The same ($r_-$) and ($r_+$) that i talk about, before! And right in the middle, there is a radius: $r_+$ is "Naria-i"! If MG is very large enough, then there is just one root at the point, means the two roots ($r_-$) and ($r_+$) collapse into one root, and that can happen at the point $r_n$ : "Naria-i" black hole (see fig: j)! Instead of working with the mass of black hole, or the schwarzschild radius of black hole (as the independent parameter here), We work with a coordinate called X.

$$X=[(r_-)-(r_+)]/R$$

X: is the difference between ($r_-$) and ($r_+$) horizon, here [($r_-$)− ($r_+$)] that entity is normalized by the size or the radius of de-sitter space "R"! And X varies between −1 to +1!

$$-1<X<1$$

When X=−1; then ($r_+$)=R (No black hole formation)! But for X=+1, when you interchange ($r_+$) and ($r_-$); ($r_-$) is always smaller than ($r_+$)! But I'm going to extend and continue the definition! So, if you interchange them ($r_+$)>($r_-$)! If you study this analytically as a function of X($r_+$; $r_-$), then [($r_+$)−($r_-$)] going to −1 to +1. So what's going on in +1??? For simplification you can imagine the cosmic horizon has shrunken down to be very small and the black hole horizon has grown to be very large! So, they interchange! The black hole horizon become cosmic horizon, and the cosmic horizon become the black hole horizon! At least the system has that kind of Symmetry! So what you may find that ΔS: The entropy difference is given by the surprisingly simple formula:

$$\Delta S=\Delta S_n\bullet[1-X^2]$$

N: stands for "naria-i" if X=0; then

$$\Delta S=\Delta S_n$$

And if you calculate the entropy difference at N,

you get $\Delta S=(1/3)\bullet S_{n\ 0}$! Here (1/3) just a numerical constant! $S_0$ is the entropy of de-sitter space at thermal equilibrium! Thats calculation is very easy to do, as there is a lot of symmetry! But if you go far from the Symmetry point the answer become very hard to defining! But it's not hard at the point N. If X=0, then according to the formula black hole shrunks into zero size, and hence there is no ΔS! Just:

$$\Delta S_n=(1/3)\bullet S_{\ 0}\ \text{(see the fig:k)*}$$



©2025 Great Britain Journals Press

Before turning into the matrix theory, lets imagine a transition! The transition start at X=−1. That's mean the Tiny-Tiny black hole in the big de-sitter space! Now let's imagine the Tiny-Tiny black hole start absorbing energy from the cosmic horizon! Now, you might be say that violet the 2nd law of Thermodynamics!

Our horizon is much colder than the black hole! So it violet the 2nd law of thermodynamics! But the 2nd law of thermodynamics not a law! It's just a statistical tendency! It's simply improbable for energy to flow from the cosmic horizon to black hole horizon! So, don't worry about! I will show you in a moment!!! But let's take that there is a boltzmann fluctuation, so energy cam flow from cosmic horizon to black hole! And in that case the black hole begin to grow! Eventually the black hole horizon and the cosmic horizon in same size at the point "N"!

But if it keep going, then cosmic horizon shrunk back and become Black Hole Horizon! Or may be no black hole at all. So, Now we find Black hole horizon become the cosmic horizon! I will called it "Inside-Out" transition (See the fig: l)*. So for an observer (see fig: m)* first the tiny black hole absorb energy from de-sitter space and grow! At some point or "N" point the both cosmic and black hole horizon at same size! And then the black hole horizon grow and become the cosmic horizon and the cosmic horizon turn into a tiny-black hole horizon! And the probability for this to happen:

$$P\_rob=e^{(-\Delta S)}$$
$$=e^{-(S_0/3)}$$

For that case: $\Delta S=\Delta S_n$

$S_0$ for big de-sitter space is a large number, so $e^{-(S_0/3)}$ is a tiny-tiny number! That is a "Boltzmann-Fluctuation"! But it still an interesting Probability for the quantum mechanics of de sitter space! Now the quest is: "Can we construct $\Delta S=\Delta S_n \bullet[1-X^2]$ for a holographic model??? The answer is yes, we can! Again it's the good-old "Matrix-Theory"

(see the fig: n)*! Dividing the system into two subsystem, means two blocks! And off-diagonal boxes are just as constraints! Consider the case of "NARIA-i" black hole! The "NARIA-i" black hole has some kind of symmetry between two blocks! It has many degrees of freedom in Big-block as in the small block! I mean two equal blocks (see fig: o)*!

That is the matrix analogou for "NARIA-i" black hole!

$$\Delta S=\sigma m\bullet(N-m) \text{ :IN MORE GENERAL CASE!!!}$$

In gravity theory S: schwarzschild radius!

$$S\sim r^2$$

$$\text{And } (r_-)=\sqrt{S_-}\ ;\ (r_+)=\sqrt{S_+}$$

$$\text{So: } X=[(r_-)-(r_+)]/R$$
$$=[(\sqrt{S_-})-(\sqrt{S_+})]/\sqrt{S_0}$$
$$=[m-(N-m)]/N$$
$$=(2m/N)-1$$

So, we have now two quantity! One is X, another is ΔS. By squaring X And rearranging Thing's little bit:


©2025 Great Britain Journals Press

$$\Delta S=\Delta S_n\bullet[1-X^2]$$

$$\Delta S_n\sim(S_0/2)\ ???$$

Now, let's talk about the dynamics of the constraints! You already know that, only "Nari-ai" black hole (m–N)=N/2 and m=N/2.

But in general according to the "BFSS"–matrix theory there are different order of degrees of freedom! And In BFSS-there is 11-Bosonic Matrices. But now assume there is a finite number of degress of freedom! But the all of them represented in block diagonal form! Now it would take some interesting dynamics to assure that if one matrix takes the block-diagonal form, all of the others also wind up [for energetic reason] in block diagonal form! I will give you an example a model, in which you can see how it can come about just by virtue of one matrix taking a block diagonal form. And also all the other takes the block diagonal form! So, that depends on the dynamics!' That's way I'm going to introduce one more matrix degree of freedom! I denoted it as "$\Re$ " (The script_R, see the fig: p)*! This matrix "$\Re$ " as same in "BFSS"–matrix theory is intended to represent the coordinate distance from the pode! In a sense that it's diagonal elements roughly speaking, it's eigen values: represent the distances (if you like, you can think in terms of Do- branes) from the center of some set of degrees of freedom or "Do-brane degrees of freedom". I'm going to write down a formula for Lagrangian l

$$L=\sum Tr(c^2R^4A^2-[\Re, A][A,\Re])+.....$$

Lagrangian is the function of some degrees of freedom, which i called A. The summation Here, over the finite number of different matrices (11-Bosonic Matrices and some number of fermionic matrices)! Here Tr represent the ordinary N×N trace! c: is just a number. R: is the size or radius of de-sitter space! And [$\Re$, A][A,$\Re$]: that represent the commutator of $\Re$ with all the degrees of freedom $A^2$. I'm not going to dicuss why it is in that way! I just represent it as a Model for how this kind of division into blocks can be dynamically explain (see the fig: q)*! The small block represent the degree of freedoms near the pode! And the big block represent the degree of freedoms near at the Horizon (*Cosmic or Black hole, whatever. See the fig: r)! If you take this form of $\Re$ and commuted with A's, then take its trace; you will find that the Lagrangian:

$$L=c^2R^4\dot{a_{ij}}\dot{a_{ji}}-R^2a_{ij}a_{ji}$$

$a_{ij}a_{ji}$ are the quadratic terms in time derevative, and $a_{ij}a_{ji}$ are quadratic terms in a's.

## III. CONCLUSION

So, what you get by this result that i finally derived? You get a system of harmonic ossicilator. If you work out the frequency of the harmonic ossicilator you may get:

$$\omega=1/cR$$

$$T=1/2\pi R$$

Suppose the frequency of the ossicilator is very large, $\omega>>T$, in other words the energy scale of the ossicilator is very large! Larger than any thing in this problem! Then you can expect this oscillations will in order to keep the energy low, you have to freeze the ossicilators into the ground state! Thats the kindvof constraints that we can imagine earlier (The off-diagonal elements are set to be zero)! The other scale of this problem is the temperature!

If we eant to know the degrees of freedom (which frozen), then what or which Temperature they frozen-out??? Thats the temperature of reaming degrees of freedom! Which roughly ~$1/2\pi R$.





©2025 Great Britain Journals Press

If $\omega >> T$, the $a_{ij}$ are frozen into ground state and carry no entropy!

If $\omega \sim T$ the $a_{ij}$ carry entropy: $\sigma - \sigma'$.

Means the off-diagonal elements $a_{ij}$ 's are not completely frozen! And instead of carrying zero entropy they will carry a entropy $\sigma - \sigma' = \Delta\sigma$.

$\sigma$: Entropy of unconstrained degrees of freedom.

$\Delta\sigma$: the entropy of "off-diagonal degrees of freedom".

*So in Case of Small Black Hole:*

$\Delta S = 2(\sigma'/\sigma) \times \sqrt{(s \bullet S)} \approx \sqrt{(s \bullet S)}$

$(\sigma'/\sigma)\_small \approx 1/2$

*For Large Black hole*

$$\Delta S = (1/2) \bullet (\sigma'/\sigma)\, S_0 (1 - X^2)$$

$$\approx (1/3) \times S_0 \bullet (1 - X^2)$$

$$(\sigma'/\sigma)\_big \approx 2/3$$

## REFERENCES


1. J. M. Maldacena, "Eternal black holes in anti-de Sitter," JHEP 04, 021 (2003) doi:10.1088/1126-6708/2003/04/021 [arXiv:hep-th/0106112 [hep-th]].
2. R. Bousso, "A Covariant entropy conjecture," JHEP 07, 004 (1999) doi:10.1088/1126-6708/1999/07/004 [arXiv:hep th/9905177 [hep-th]].
3. W. Fischler and L. Susskind, "Holography and cosmology," [arXiv:hep-th/9806039 [hep-th]].
4. J. Maldacena, D. Stanford and Z. Yang, "Conformal symmetry and its breaking in two dimensional Nearly Anti-de-Sitter space," PTEP 2016, no.12, 12C104 (2016) doi:10.1093/ptep/ptw124 [arXiv:1606.01857 [hep-th]].
5. H. W. Lin, J. Maldacena and Y. Zhao, "Symmetries Near the Horizon," JHEP 08, 049 (2019) doi:10.1007/JHEP08(2019)049 [arXiv:1904.12820 [hep-th]].
6. T. Banks, B. Fiol and A. Morisse, "Towards a quantum theory of de Sitter space," JHEP 12, 004 (2006) doi:10.1088/1126- 6708/2006/12/004 [arXiv:hep-th/0609062 [hep-th]].
7. L. Susskind, "Addendum to Fast Scramblers," [arXiv:1101.6048 [hep-th]].
8. T. Banks and W. Fischler, "Holographic Space-time, Newton's Law and the Dynamics of Black Holes," [arXiv:1606.01267 [hep-th]].
9. J. S. Cotler, G. Gur-Ari, M. Hanada, J. Polchinski, P. Saad, S. H. Shenker, D. Stanford, A. Streicher and M. Tezuka, "Black Holes and Random Matrices," JHEP 05, 118 (2017) [erra tum: JHEP 09, 002 (2018)] doi:10.1007/JHEP05(2017)118 [arXiv:1611.04650 [hep-th]].
10. P. Saad, S. H. Shenker and D. Stanford, "A semiclassical ramp in SYK and in gravity," [arXiv:1806.06840 [hep-th]].
11. P. Saad, "Black holes, baby universes, and random matrices,"
12. D. Marolf and H. Maxfield, "Transcending the ensemble: baby universes, spacetime wormholes, and the order and disorder of black hole information," JHEP 08, 044 (2020) doi:10.1007/JHEP08(2020)044 [arXiv:2002.08950 [hep-th]].





©2025 Great Britain Journals Press

13. A. Almheiri, R. Mahajan, J. Maldacena and Y. Zhao, "The Page curve of Hawking radiation from semiclassical geom-etry," JHEP 03, 149 (2020) doi:10.1007/JHEP03(2020)149 [arXiv:1908.10996 [hep-th]].
14. S. W. Hawking and I. G. Moss, "Supercooled Phase Transitions in the Very Early Universe," Phys. Lett. B 110, 35-38 (1982) doi:10.1016/0370-2693(82)90946-7
15. E. J. Weinberg, "Hawking-Moss bounces and vac-uum decay rates," Phys. Rev. Lett. 98, 251303 (2007) doi:10.1103/PhysRevLett.98.251303 [arXiv:hep-th/0612146 [hep-th]].
16. T. Banks, W. Fischler and S. Paban, "Recurrent night-mares? Measurement theory in de Sitter space,"JHEP 12, 062 (2002) doi:10.1088/1126-6708/2002/12/062 [arXiv:hep-th/0210160 [hep-th]].

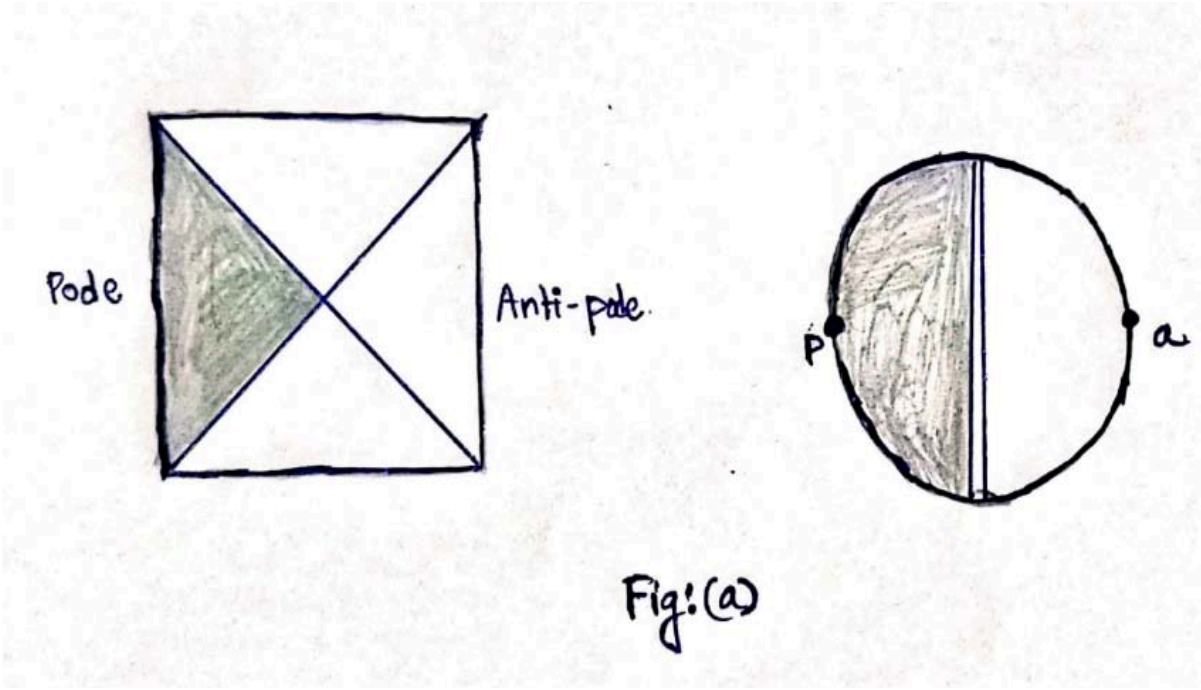


Fig:(a)

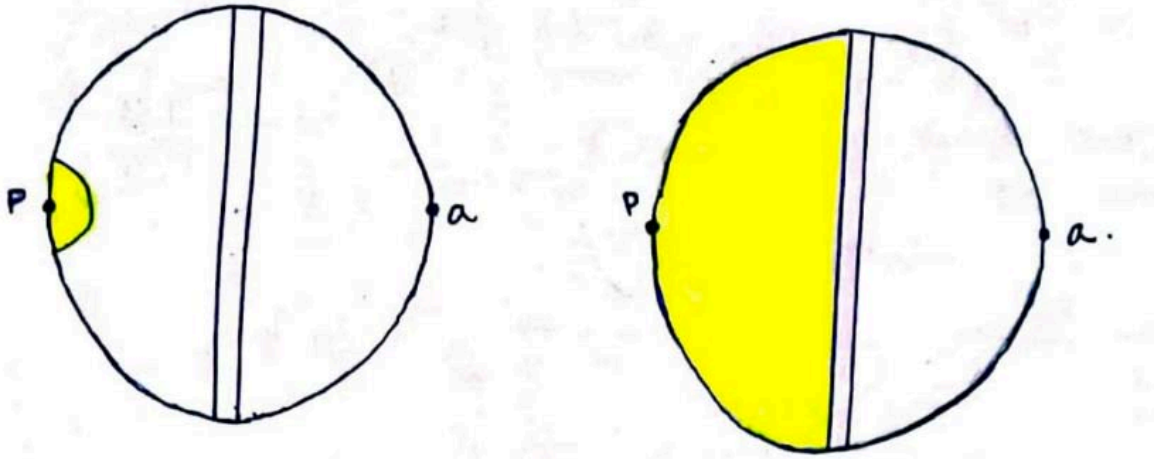


HOLOGRAPHIC DOF AT STREATCHED HORIZON (Fig:b)





©2025 Great Britain Journals Press

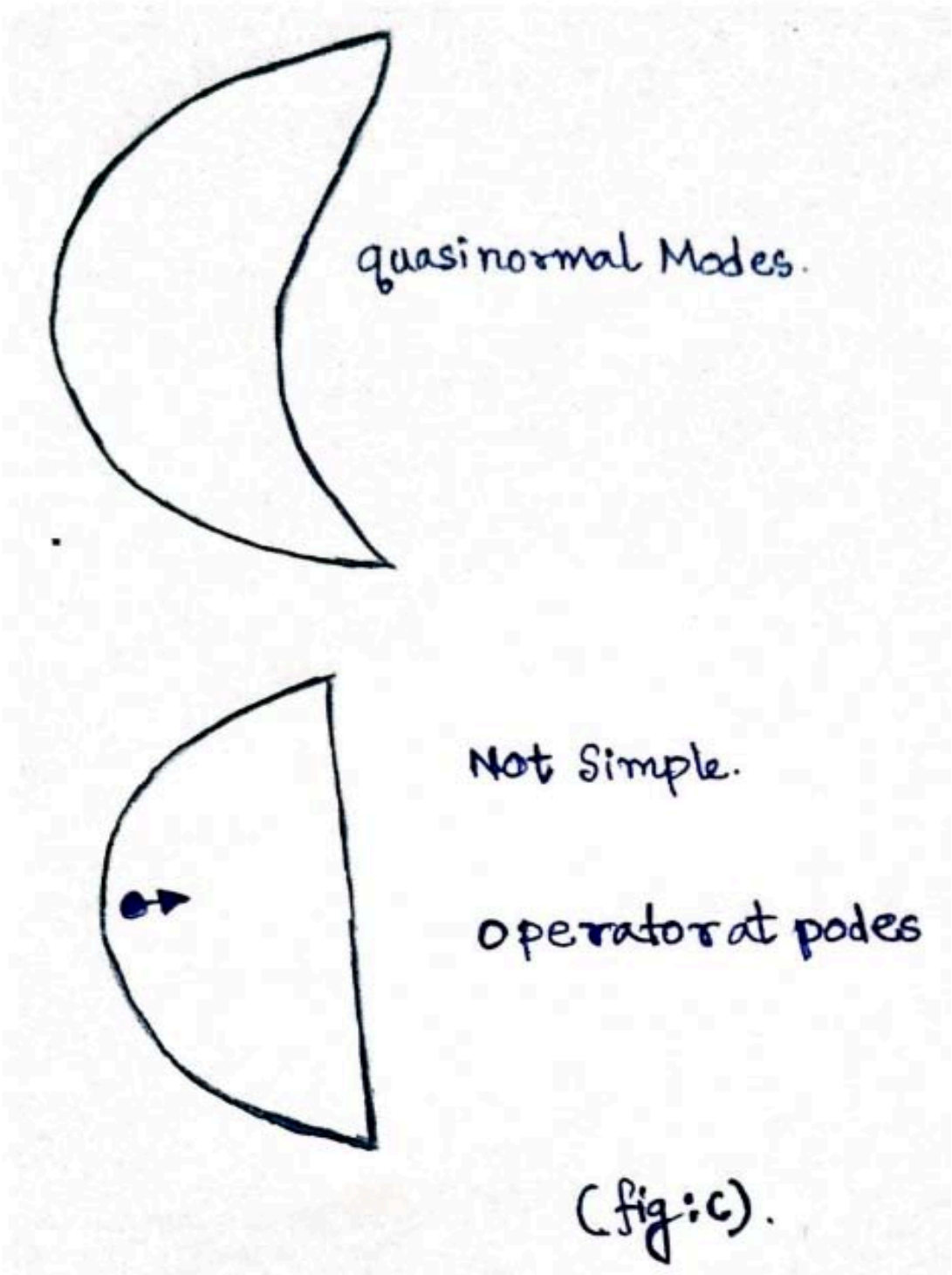



©2025 Great Britain Journals Press

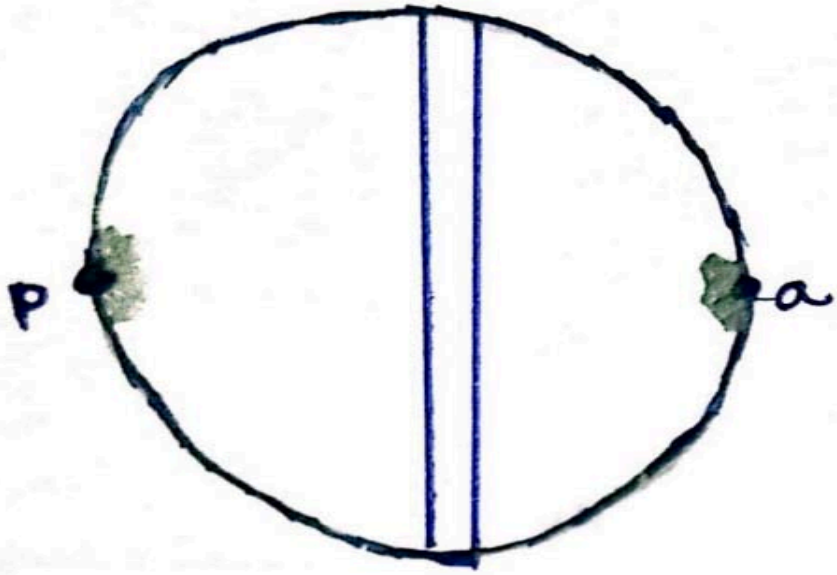


fig:(d)

## SMALL BLACK HOLES

$[\delta << S_0]$

$2MG << R$

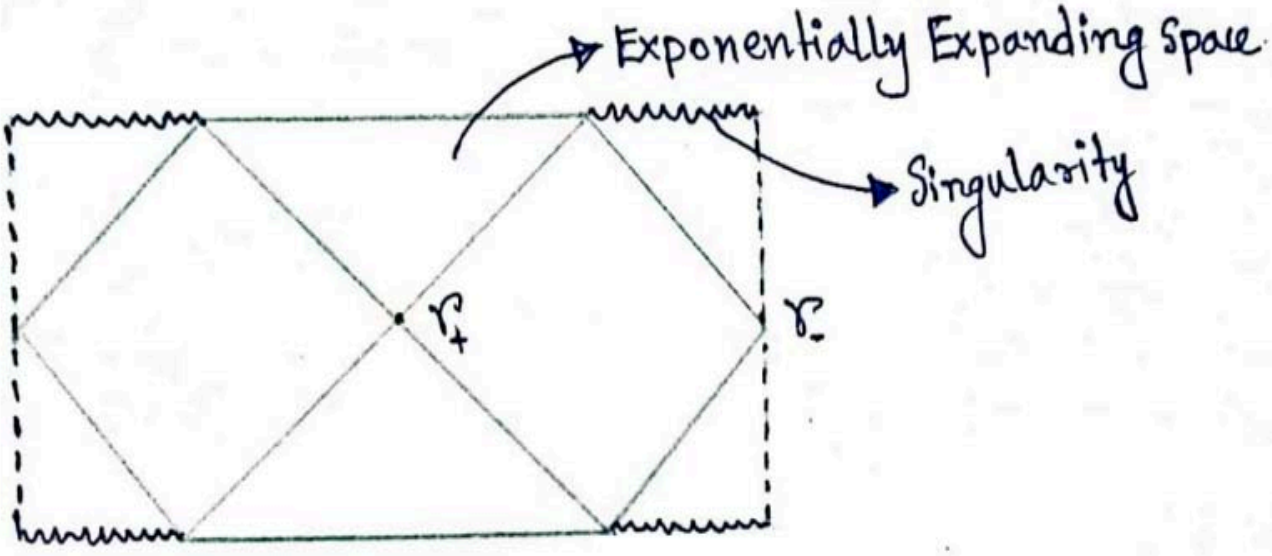


fig:(e)





©2025 Great Britain Journals Press

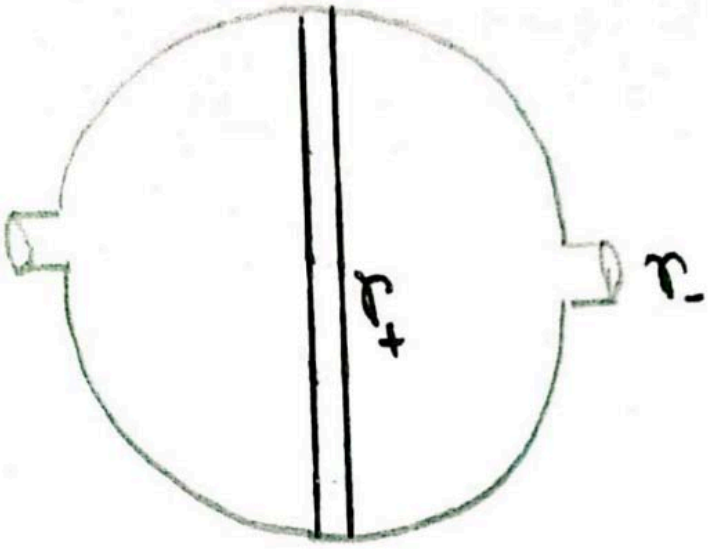


fig: (f)

DOF = FINITE

# MATRAICES!

$$A = \begin{bmatrix} a_{11} & a_{12} & a_{13} \cdots\cdots a_{1n} \\ a_{21} & \ddots & \\ \vdots & & \ddots \\ \vdots & & \ddots \\ \vdots & & \ddots \\ a_{n1} & & \end{bmatrix} ; \; S_0 = \sigma N^2$$

fig: (g)


©2025 Great Britain Journals Press

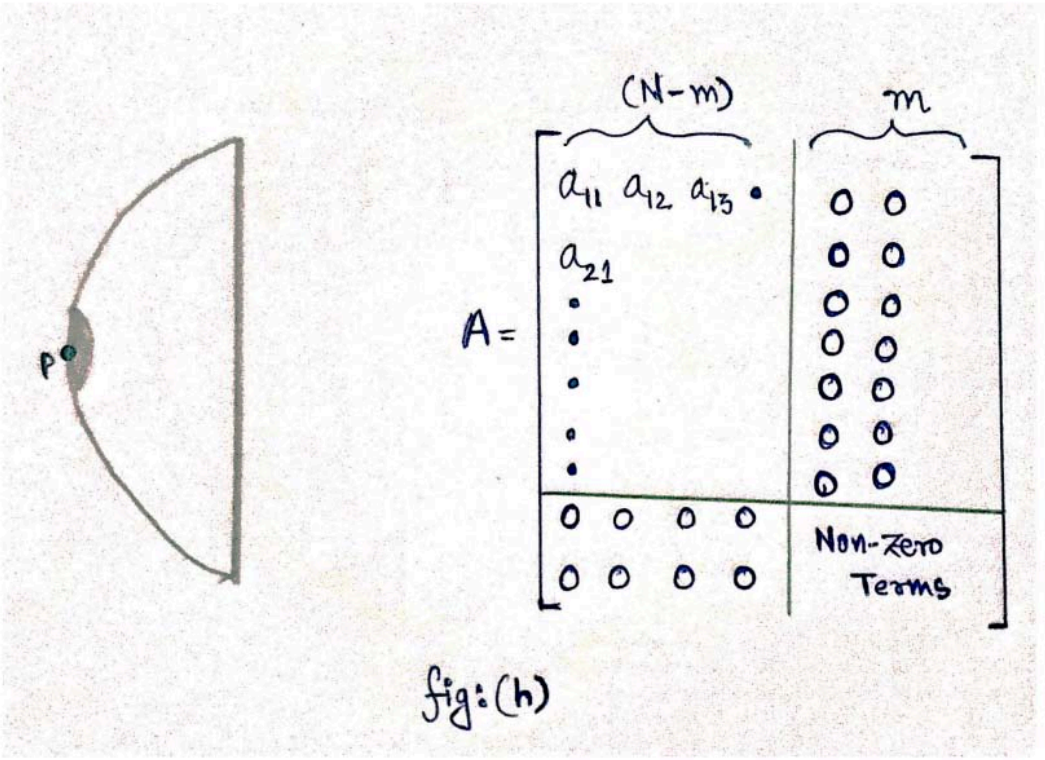


fig: (h)

## TOY - MODEL

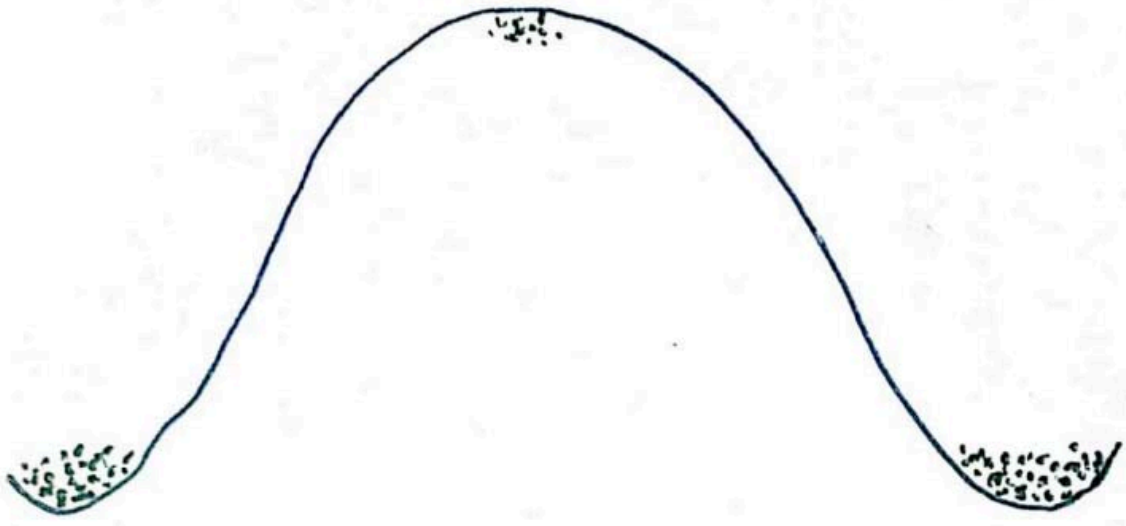

fig: (i)





©2025 Great Britain Journals Press

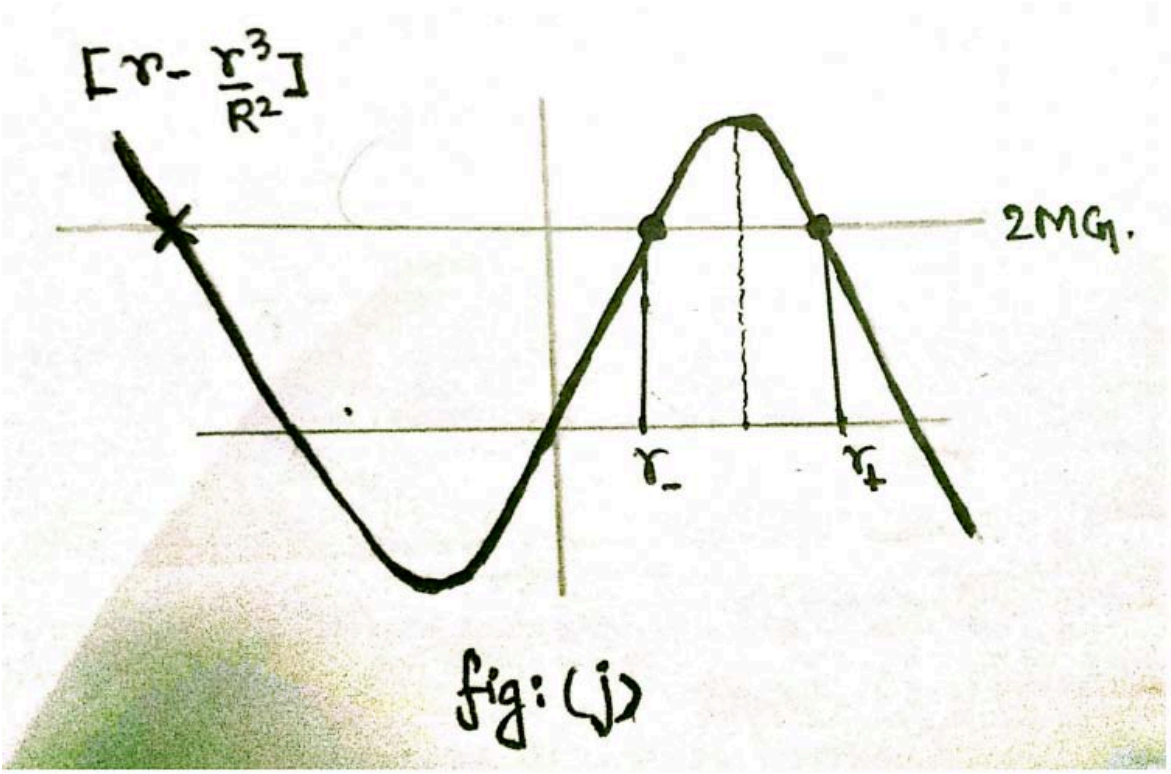


fig: (j)

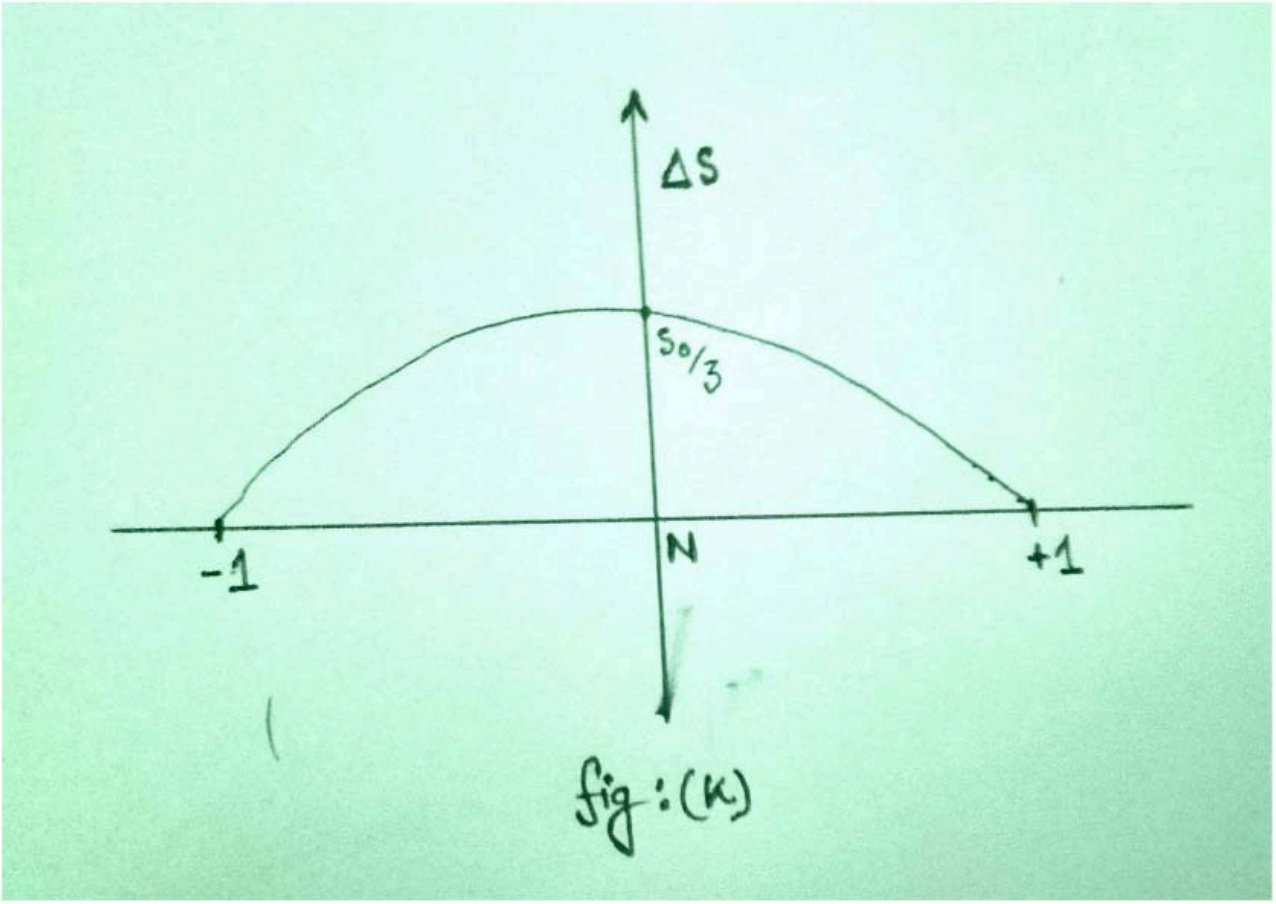


fig: (k)


©2025 Great Britain Journals Press

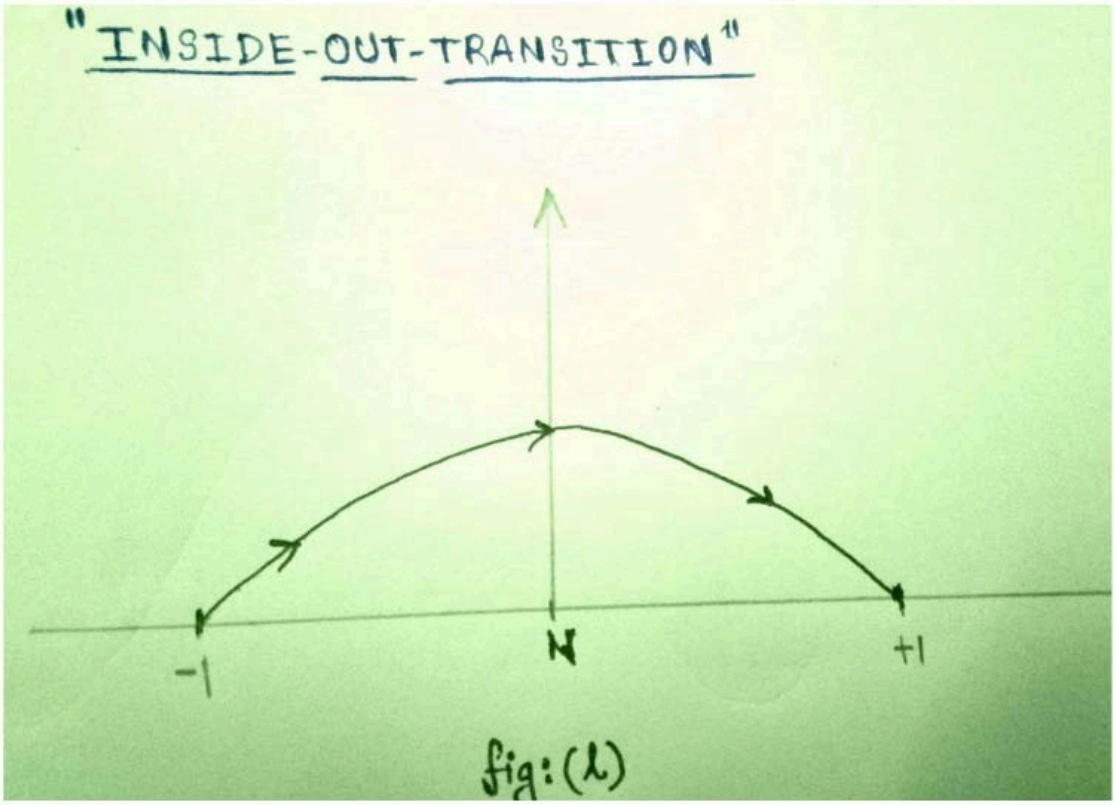


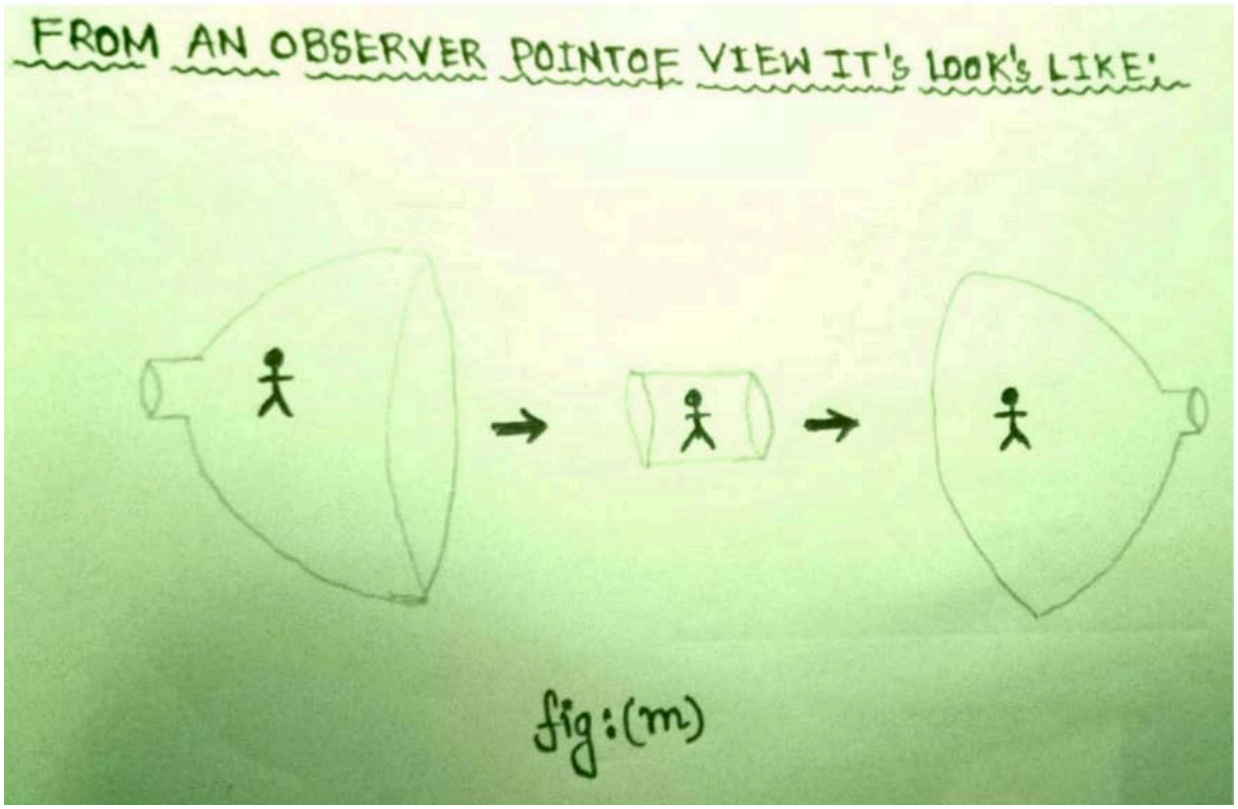






©2025 Great Britain Journals Press

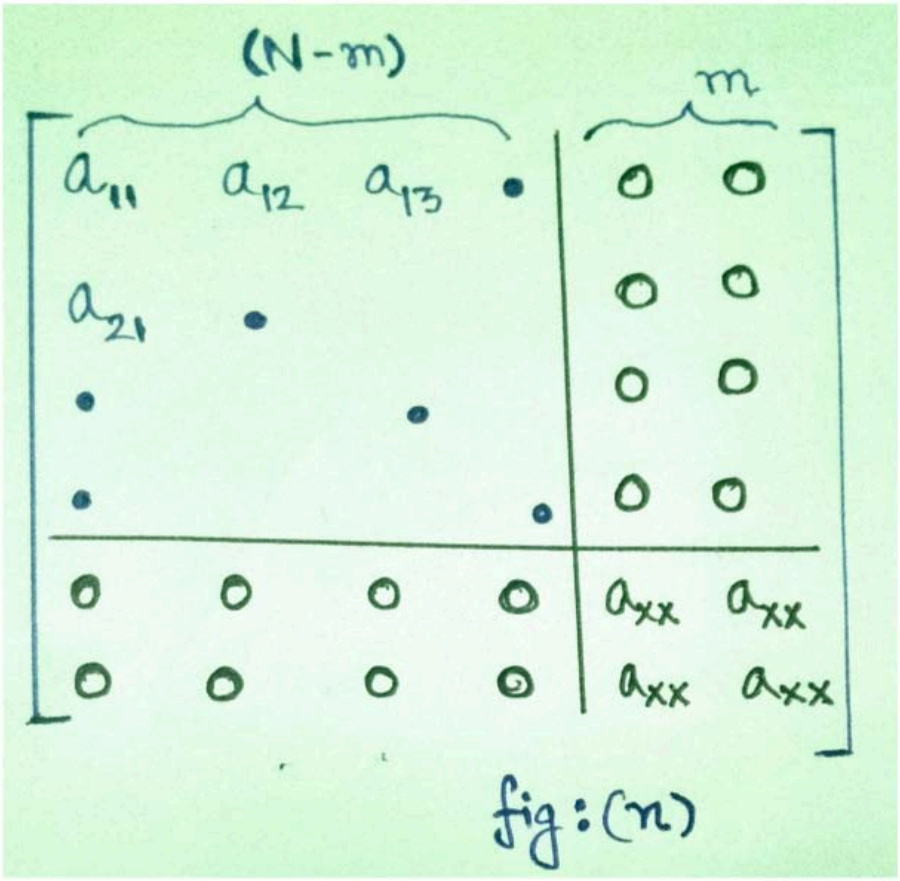


fig: (n)

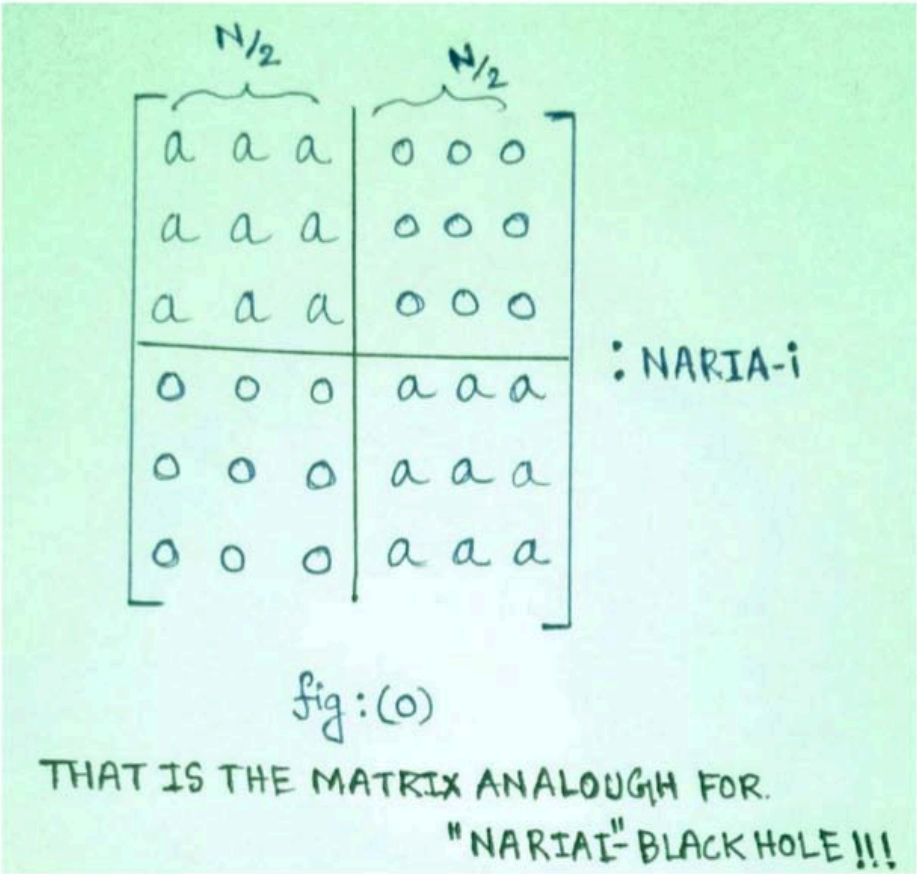


fig: (o)

THAT IS THE MATRIX ANALOUGH FOR.
"NARIAI" BLACK HOLE !!!


©2025 Great Britain Journals Press

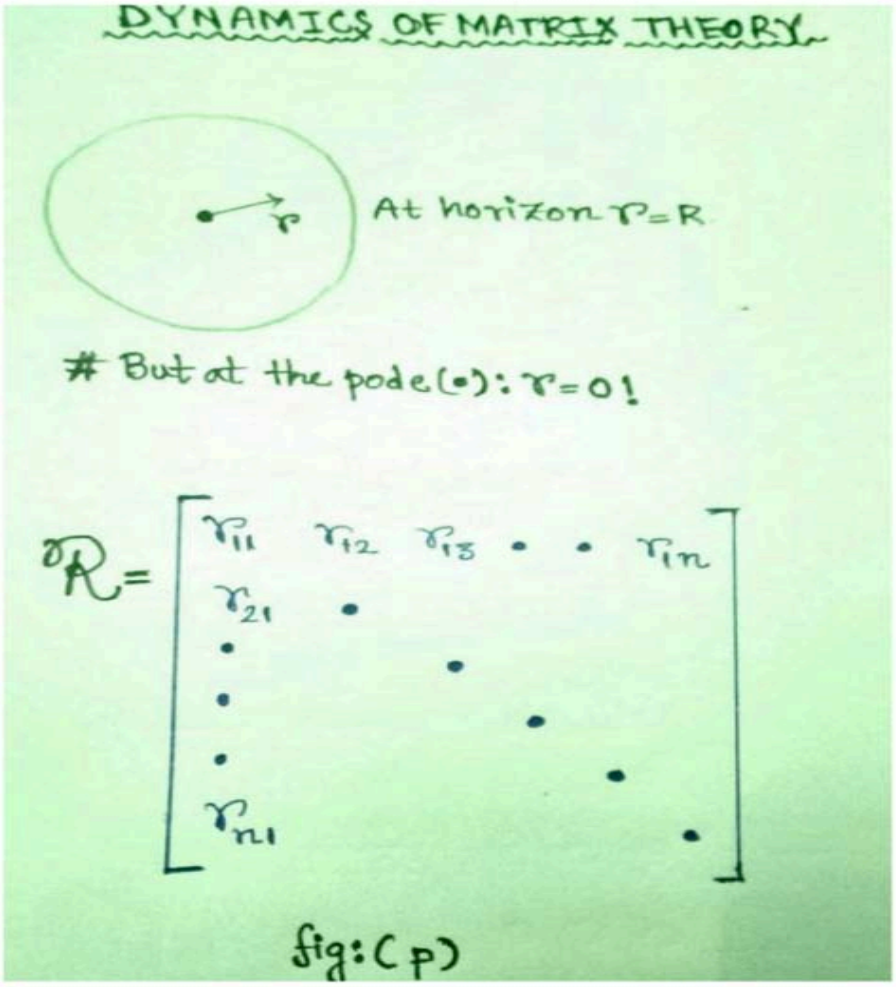


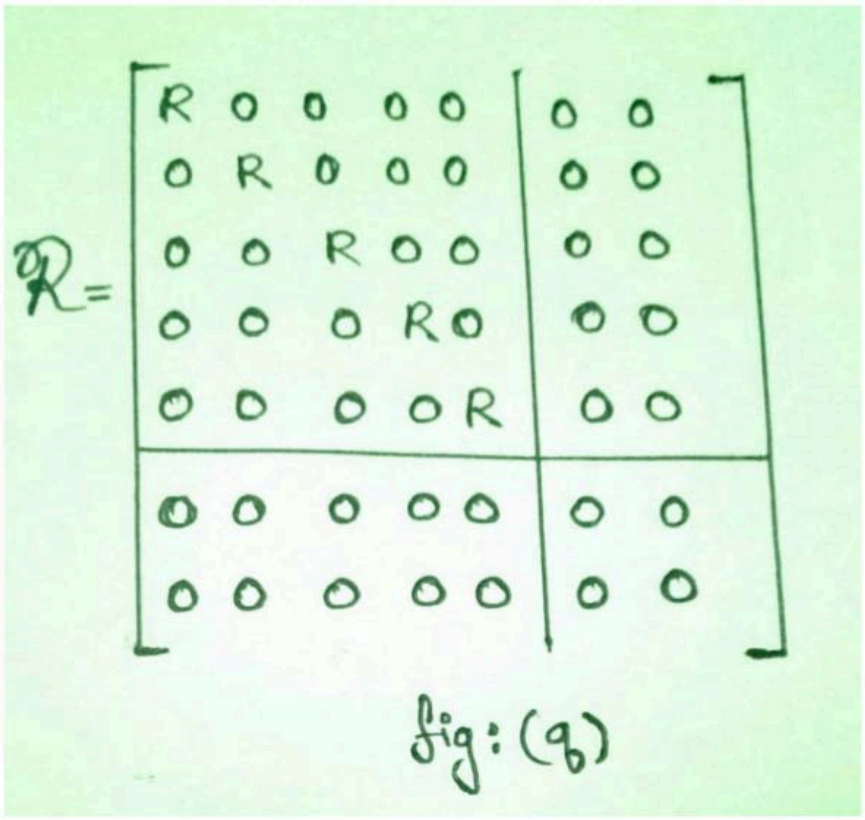






©2025 Great Britain Journals Press



©2025 Great Britain Journals Press

Scan to know paper details and
author's profile

# Analysis and Control of a Mastitis Dynamic Model

*Lakshmi. N. Sridhar*

*Department University of Puerto*

## ABSTRACT

In this study, bifurcation analysis and multi-objective nonlinear model predictive control are performed on a mastitis dynamic model . Bifurcation analysis is a powerful mathematical tool used to deal with the nonlinear dynamics of any process. Several factors must be considered, and multiple objectives must be met simultaneously. The MATLAB program MATCONT was used to perform the bifurcation analysis. The MNLMPC calculations were performed using the optimization language PYOMO in conjunction with the state-of-the-art global optimization solvers IPOPT and BARON. The bifurcation analysis revealed a branch point. The MNLMC converged on the Utopia solution. The branch point (which causes multiple steady-state solutions from a singular point) is very beneficial because it enables the Multiobjective nonlinear model predictive control calculations to converge to the Utopia point (the best possible solution) in the model.

*Keywords:* bifurcation, optimization, control, mastitis.

*Classification:* LCC Code: QA614.8

*Language:* English

Great Britain Journals Press

LJP Copyright ID: 925618
Print ISSN: 2631-8490
Online ISSN: 2631-8504

London Journal of Research in Science: Natural & Formal

Volume 25 | Issue 15 | Compilation 1.0

© 2025. Lakshmi. N. Sridhar. This is a research/review paper, distributed under the terms of the Creative Commons Attribution-Noncom-mercial 4.0 Unported License http://creativecommons.org/licenses/by-nc/4.0/), permitting all noncommercial use, distribution, and reproduction in any medium, provided the original work is properly cited.

# Analysis and Control of a Mastitis Dynamic Model

Lakshmi. N. Sridhar

## ABSTRACT

*In this study, bifurcation analysis and multi-objective nonlinear model predictive control are performed on a mastitis dynamic model . Bifurcation analysis is a powerful mathematical tool used to deal with the nonlinear dynamics of any process. Several factors must be considered, and multiple objectives must be met simultaneously. The MATLAB program MATCONT was used to perform the bifurcation analysis. The MNLMPC calculations were performed using the optimization language PYOMO in conjunction with the state-of-the-art global optimization solvers IPOPT and BARON. The bifurcation analysis revealed a branch point. The MNLMC converged on the Utopia solution. The branch point (which causes multiple steady-state solutions from a singular point) is very beneficial because it enables the Multiobjective nonlinear model predictive control calculations to converge to the Utopia point (the best possible solution) in the model.*

*Keywords:* bifurcation, optimization, control, mastitis.

*Author:* Chemical Engineering Department University of Puerto Rico Mayaguez, PR 00681.

## I. BACKGROUND

Mastitis is an inflammatory condition of the mammary gland that affects both humans and animals, particularly dairy cattle, and is a significant concern in veterinary and human medicine. The condition can occur as a result of infection, physical injury, or other irritations to the mammary tissue. In dairy cows, mastitis is among the most costly and prevalent diseases, leading to reduced milk production, alterations in milk composition, and economic losses for farmers. In humans, mastitis most often affects lactating women, a condition known as lactational mastitis, though it can also occur in non-lactating individuals. Understanding mastitis involves examining its causes, symptoms, diagnosis, treatment, prevention, and impact on public health and the agricultural economy.

Mastitis is primarily caused by bacterial infection. The most common pathogens include *Staphylococcus aureus*, *Streptococcus agalactiae*, *Streptococcus uberis*, and *Escherichia coli*. These bacteria can enter the mammary gland through the teat canal, especially when the natural defense barriers of the udder are compromised. Factors such as poor milking hygiene, mechanical injuries, improper milking machine maintenance, or environmental exposure to contaminated bedding can facilitate bacterial entry. Once inside the mammary gland, the bacteria multiply and trigger an immune response, leading to inflammation, swelling, pain, and altered milk secretion. In some cases, fungi, viruses, or mycoplasmas can also be involved, although bacterial infections remain the predominant cause.

In dairy cattle, mastitis is typically classified into two forms: clinical and subclinical. Clinical mastitis is easily recognizable because of visible signs in the udder and milk. The affected quarter of the udder becomes swollen, hot, painful, and sometimes hard. The milk may appear watery, clotted, or contain flakes and pus. The cow might show systemic symptoms such as fever, reduced appetite, and decreased milk yield. Subclinical mastitis, on the other hand, is more insidious and often goes unnoticed because there are no visible symptoms. However, it leads to reduced milk production and altered milk

London Journal of Research in Science: Natural & Formal

©2025 Great Britain Journals Press

composition. Subclinical mastitis can persist for long periods and serve as a reservoir of infection, spreading pathogens to other cows through milking equipment or handlers. Because of its hidden nature, subclinical mastitis is often more economically damaging than the clinical form.

In humans, mastitis most commonly occurs in breastfeeding women, usually within the first few weeks after childbirth. This form of mastitis, known as lactational or puerperal mastitis, results from milk stasis — the accumulation of milk within the breast due to infrequent feeding, poor latch, or blocked ducts. The stagnant milk serves as a medium for bacterial growth, often involving *Staphylococcus aureus* or *Streptococcus* species. The condition presents with breast pain, swelling, redness, warmth, and fever. In severe cases, abscess formation can occur if the infection is not promptly treated. Non-lactational mastitis can also affect women or men and may be associated with smoking, nipple piercing, or underlying conditions such as duct ectasia or diabetes.

Diagnosis of mastitis involves clinical examination and laboratory analysis of milk or tissue samples. In dairy cows, the California Mastitis Test (CMT) is commonly used as a rapid, on-farm diagnostic tool to detect subclinical cases. This test measures the somatic cell count (SCC) — a key indicator of udder inflammation — in the milk. A high SCC reflects the presence of immune cells responding to infection. For more definitive diagnosis, bacteriological culture and antibiotic sensitivity testing can identify the causative organisms and guide treatment decisions. In human mastitis, diagnosis is usually based on symptoms and physical examination, though ultrasound or aspiration may be used to rule out abscess formation.

Treatment of mastitis depends on the cause and severity of the condition. In dairy cattle, antibiotic therapy is the most common approach, often administered through intramammary infusion. The choice of antibiotic must consider the causative bacteria, the severity of infection, and milk withdrawal periods to prevent antibiotic residues in milk intended for human consumption. In addition to antibiotics, supportive therapies such as anti-inflammatory drugs, frequent milking, and proper hydration help reduce inflammation and restore milk flow. In human cases, management involves continued breastfeeding or milk expression to relieve engorgement, along with antibiotic therapy if infection is suspected. Pain relief through warm compresses, gentle massage, and rest are also recommended. If an abscess forms, surgical drainage may be necessary.

Prevention of mastitis is far more effective and economical than treatment. In dairy herds, mastitis control programs focus on hygiene, proper milking procedures, and herd management. Key preventive measures include maintaining clean milking equipment, using pre- and post-milking teat disinfectants, ensuring good cow housing conditions, and promptly treating any teat injuries. Cows with chronic or recurrent mastitis may need to be culled to prevent spreading infection. Regular monitoring of somatic cell counts and routine screening using tests like the CMT can help identify and control subclinical cases early. In humans, prevention focuses on ensuring proper breastfeeding techniques, frequent feeding to prevent milk stasis, and maintaining nipple hygiene.

The economic and public health implications of mastitis are substantial. In the dairy industry, mastitis leads to direct losses from decreased milk yield and quality, veterinary costs, and discarded milk due to antibiotic contamination. Indirect losses include reduced reproductive efficiency, premature culling of affected cows, and the cost of implementing control programs. Mastitis also affects milk composition by reducing fat, lactose, and casein content, which in turn lowers its suitability for processing into dairy products such as cheese and yogurt. On a global scale, mastitis contributes to significant financial losses running into billions of dollars annually. For human health, although lactational mastitis is generally treatable, it can cause significant discomfort, psychological distress, and interruption of breastfeeding, affecting both mother and infant nutrition.




©2025 Great Britain Journals Press

Recent research in mastitis management has focused on developing alternative therapies and improving diagnostic tools. With growing concerns over antibiotic resistance, scientists are exploring non-antibiotic approaches such as vaccines, probiotics, bacteriophages, and herbal remedies. Vaccines against *Staphylococcus aureus* and *E. coli* have shown promise in reducing the incidence and severity of infection, though they are not yet universally effective. The use of automated milking systems and data-driven herd management has also enhanced early detection and control of mastitis. Advances in molecular biology have enabled rapid identification of pathogens through polymerase chain reaction (PCR) and other genomic tools, providing faster and more precise diagnostic capabilities.

Mastitis is a multifactorial disease that remains a major concern in both animal and human health. It involves complex interactions between pathogens, host defenses, and environmental factors. While it is most often associated with bacterial infection, underlying management practices and hygiene conditions play a critical role in determining susceptibility. Effective control and prevention require a comprehensive approach that combines good husbandry, prompt detection, appropriate treatment, and ongoing research into new solutions. For the dairy industry, maintaining udder health is essential not only for economic sustainability but also for ensuring the quality and safety of milk. In human health, timely management of mastitis ensures continued breastfeeding, maternal well-being, and infant nutrition. Despite advances in understanding and technology, mastitis continues to challenge veterinarians, farmers, and healthcare providers, underscoring the need for continued vigilance and innovation in its control.

Lam et al (1996)[1] used mathematical models to estimate the efficacy of post-milking teat disinfection in split-udder trials of dairy cows. Cherry et al (1998)[2] evaluated the bovine viral diarrhea virus control using a mathematical model of infection dynamics. Hamann(2005)[3] discussed the diagnosis of Mastitis and Indicators of milk quality. Dorte et al (2010)[4] modelled the dynamics of intramammary E. coli infections in dairy cows. Michelle et al (2016)[5] modelled antimicrobial resistance in agricultural waste. Cobirka et al (2020)[6] researched the epidemiology and classification of mastitis. Abera (2020)[7] , did a review on the prevalence and associated risk factors of bovine mastitis in lactating cows of smallholder dairy farms in Ethiopia. Izneid et al. (2023)[8] developed an optimal control strategy for a mathematical model of mastitis dynamics.

This work aims to perform bifurcation analysis and multiobjective nonlinear control (MNLMPC) studies on a Mastitis dynamic model described in Izneid et l (2023)[8] . The paper is organized as follows. First, the model equations are presented, followed by a discussion of the numerical techniques involving bifurcation analysis and multiobjective nonlinear model predictive control (MNLMPC). The results are then presented, followed by the discussion and conclusions.

## II. MODEL EQUATIONS

The bacteria population is represented by bv. The cattle populations are divided into four classes: the susceptible class (sv), subclinical class (cs), which includes active cattle that do not produce noticeable symptoms of mastitis, clinical class (cv ); which represents all cattle that are showing the symptoms of mastitis, and the recovered class (rv).

$\gamma$ is the ingestion rate, and K is the concentration of Staphylococcus and Streptococcus bacteria in the environment. p represents the probability of the susceptible cattle becoming clinically infected. The subclinical cattle develop mastitis and join the clinical class at a rate $\phi$ and others join the recovered class at a rate $\theta$. The rate at which the cattle go from clinical to recovered class is $\delta$. $\xi, \mu$ are the disease-induced mortality rate and the natural death rate of the individuals.



©2025 Great Britain Journals Press

The subclinical/clinical cattle population increases the bacteria in the environment at a rate $\beta 1, \beta 2$. $\mu b$ represents the bacteria's death rate. The control parameters u1, u2, and u3 represent the preventive measures, the screening of subclinical individuals, and the treatment of clinical individuals. The model equations are

$$\lambda = \frac{bv(\gamma)}{(k+bv)}$$

$$\frac{d(sv)}{dt} = \pi + \alpha(rv) - (1-u1)(\lambda)sv - \mu(sv)$$

$$\frac{d(cs)}{dt} = (1-u1)(1-p)\lambda(sv) - (u2+\phi)cs - (\theta + \beta 1 + \mu + \xi)cs$$

$$\frac{d(cv)}{dt} = (1-u1)(p)\lambda(sv) + (1-u2)\phi(cs) - (u3+\delta)cv - (\beta 2 + \mu + \xi)cv$$

$$\frac{d(rv)}{dt} = \theta(cs) + (u2+\delta)cv - (\alpha + mu)rv$$

$$\frac{d(bv)}{dt} = \beta 1(cs) + \beta 2(cv) - \mu b(bv)$$

The base parameters are $\pi$ =500; mu $\mu$ =0.02; $\alpha$ =0.99; $\gamma$ =0.09; p=0.6; k=1000; $\xi$ =0.9992;

$\delta$ =0.998; $\phi$ =0.999; $\theta$ =0.98; $\beta 1$ =0.009; $\beta 2$ =0.008; $\mu b$ =0.01; u1=0; u2=0; u3=0;

## III. BIFURCATION ANALYSIS

The MATLAB software MATCONT is used to perform the bifurcation calculations. Bifurcation analysis deals with multiple steady-states and limit cycles. Multiple steady states occur because of the existence of branch and limit points. Hopf bifurcation points cause limit cycles. A commonly used MATLAB program that locates limit points, branch points, and Hopf bifurcation points is MATCONT(Dhooge, Govaerts, and Kuznetsov, 2003[9]; Dhooge, Govaerts, Kuznetsov, Mestrom and Riet, 2004[10] ). This program detects Limit points(LP), branch points(BP), and Hopf bifurcation points(H) for an ODE system

$$\frac{dx}{dt} = f(x, \alpha)$$

$x \in R^n$ Let the bifurcation parameter be $\alpha$. Since the gradient is orthogonal to the tangent vector,

The tangent plane at any point $w = [w_1, w_2, w_3, w_4, ....w_{n+1}]$ must satisfy

$$Aw = 0$$

Where A is

$$A = [\partial f / \partial x \quad | \partial f / \partial \alpha]$$


©2025 Great Britain Journals Press

where $\partial f / \partial x$ is the Jacobian matrix. For both limit and branch points, the Jacobian matrix $J = [\partial f / \partial x]$ must be singular.

For a limit point, there is only one tangent at the point of singularity. At this singular point, there is a single non-zero vector, y, where Jy=0. This vector is of dimension n. Since there is only one tangent the vector

$y = (y_1, y_2, y_3, y_4, ...y_n)$ must align with $\hat{w} = (w_1, w_2, w_3, w_4, ...w_n)$ . Since

$$J\hat{w} = Aw = 0$$

the n+1 th component of the tangent vector $w_{n+1}$ = 0 at a limit point (LP).

For a branch point, there must exist two tangents at the singularity. Let the two tangents be z and w. This implies that

$$Az = 0$$
$$Aw = 0$$

Consider a vector v that is orthogonal to one of the tangents (say w). v can be expressed as a linear combination of z and w ( $v = \alpha z + \beta w$ ). Since $Az = Aw = 0$ ; $Av = 0$ and since w and v are orthogonal,

$w^T v = 0$ . Hence $Bv = \begin{bmatrix} A \\ w^T \end{bmatrix} v = 0$ which implies that B is singular.

Hence, for a branch point (BP) the matrix $B = \begin{bmatrix} A \\ w^T \end{bmatrix}$ must be singular.

At a Hopf bifurcation point,

$$\det(2f_x(x,\alpha)@I_n) = 0$$

@ indicates the bialternate product while $I_n$ is the n-square identity matrix. Hopf bifurcations cause limit cycles and should be eliminated because limit cycles make optimization and control tasks very difficult. More details can be found in Kuznetsov (1998[11]; 2009[12]) and Govaerts (2000) [13].

## IV. MULTIOBJECTIVE NONLINEAR MODEL PREDICTIVE CONTROL(MNLMPC)

The rigorous multiobjective nonlinear model predictive control (MNLMPC) method developed by Flores Tlacuahuaz et al (2012)[14] was used.

Consider a problem where the variables $\sum_{t_i=0}^{t_i=t_f} q_j(t_i)$ (j=1, 2..n) have to be optimized simultaneously for a dynamic problem





©2025 Great Britain Journals Press

$$\frac{dx}{dt} = F(x,u)$$

$t_f$ being the final time value, and n the total number of objective variables and u the control parameter. The single objective optimal control problem is solved individually optimizing each of the variables $\sum_{t_j=0}^{t_i=t_f} q_j(t_i)$ The optimization of $\sum_{t_{i=0}}^{t_i=t_f} q_j(t_i)$ will lead to the values $q_j^*$. Then, the multiobjective optimal control (MOOC) problem that will be solved is

$$\min(\sum_{j=1}^{n}(\sum_{t_{i=0}}^{t_i=t_f} q_j(t_i) - q_j^*))^2$$

$$subject\ to\ \frac{dx}{dt} = F(x,u);$$

This will provide the values of u at various times. The first obtained control value of u is implemented and the rest are discarded. This procedure is repeated until the implemented and the first obtained control values are the same or if the Utopia point where ( $\sum_{t_{i=0}}^{t_i=t_f} q_j(t_i) = q_j^*$ for all j) is obtained.

Pyomo (Hart et al, 2017)[15] is used for these calculations. Here, the differential equations are converted to a Nonlinear Program (NLP) using the orthogonal collocation method The NLP is solved using IPOPT (Wächter And Biegler, 2006)[16]and confirmed as a global solution with BARON (Tawarmalani, M. and N. V. Sahinidis 2005)[17].

1. The steps of the algorithm are as follows
2. Optimize $\sum_{t_{i=0}}^{t_i=t_f} q_j(t_i)$ and obtain $q_j^*$.
3. Minimize $(\sum_{j=1}^{n}(\sum_{t_{i=0}}^{t_i=t_f} q_j(t_i) - q_j^*))^2$ and get the control values at various times.
4. Implement the first obtained control values

Repeat steps 1 to 3 until there is an insignificant difference between the implemented and the first obtained value of the control variables or if the Utopia point is achieved. The Utopia point is when

$$\sum_{t_{i=0}}^{t_i=t_f} q_j(t_i) = q_j^* \text{ for all j.}$$

Sridhar (2024)[18] demonstrated that when the bifurcation analysis revealed the presence of limit and branch points tthe MNLMPC calculations to converge to the Utopia solution . For this, the singularity condition, caused by the presence of the limit or branch points was imposed on the co-state equation (Upreti, 2013)[19]. If the minimization of $q_1$ lead to the value $q_1^*$ and the minimization of $q_2$ lead


©2025 Great Britain Journals Press

to the value $q_2^*$ The MNLPMC calculations will minimize the function $(q_1 - q_1^*)^2 + (q_2 - q_2^*)^2$. The multiobjective optimal control problem is

$$\min \quad (q_1 - q_1^*)^2 + (q_2 - q_2^*)^2 \quad subject\ to \ \frac{dx}{dt} = F(x,u)$$

Differentiating the objective function results in

$$\frac{d}{dx_i}((q_1 - q_1^*)^2 + (q_2 - q_2^*)^2) = 2(q_1 - q_1^*)\frac{d}{dx_i}(q_1 - q_1^*) + 2(q_2 - q_2^*)\frac{d}{dx_i}(q_2 - q_2^*)$$

The Utopia point requires that both $(q_1 - q_1^*)$ and $(q_2 - q_2^*)$ are zero. Hence

$$\frac{d}{dx_i}((q_1 - q_1^*)^2 + (q_2 - q_2^*)^2) = 0$$

The optimal control co-state equation (Upreti; 2013)[43] is

$$\frac{d}{dt}(\lambda_i) = -\frac{d}{dx_i}((q_1 - q_1^*)^2 + (q_2 - q_2^*)^2) - f_x\lambda_i; \quad \lambda_i(t_f) = 0$$

$\lambda_i$ is the Lagrangian multiplier. $t_f$ is the final time. The first term in this equation is 0, and hence

$$\frac{d}{dt}(\lambda_i) = -f_x\lambda_i; \lambda_i(t_f) = 0$$

At a limit or a branch point, for the set of ODE $\frac{dx}{dt} = f(x,u)$ $f_x$ is singular. Hence there are two different vectors-values for $[\lambda_i]$ where $\frac{d}{dt}(\lambda_i) > 0$ and $\frac{d}{dt}(\lambda_i) < 0$. In between there is a vector $[\lambda_i]$ where $\frac{d}{dt}(\lambda_i) = 0$ . This coupled with the boundary condition $\lambda_i(t_f) = 0$ will lead to $[\lambda_i] = 0$ This makes the problem an unconstrained optimization problem, and the optimal solution is the Utopia solution.

## I. RESULTS AND DISCUSSION

When $\theta$ is the bifurcation parameter, a branch point is located at (sv, cs, cv, rv, bv, $\theta$) values of ( 25000, 0, 0, 0, 0, 0.469300 )(Fig. 1a).

For the MNLMPC, u1, u u3 are the control parameters, and $\sum_{t_i=0}^{t_i=t_f} cv(t_i), \sum_{t_i=0}^{t_i=t_f} cs(t_i)$ were minimized individually, and each led to a value of 0. The overall optimal control problem will involve the





©2025 Great Britain Journals Press

minimization of $(\sum_{t_i=0}^{t_i=t_f} cv(t_i)-0)^2+(\sum_{t_i=0}^{t_i=t_f} cs(t_i)-0)^2$ was minimized subject to the equations governing the model. This led to a value of zero (the Utopia point). The MNLMPC values of the control variables, u1, u2, and u3 were 0.202, 0.454, 0.465. The MNLMPC profiles are shown in Figs 2a-2d. The control profiles of u1, u2, and u3 exhibited noise (Fig. 2c) and this was remedied using the Savitzky-Golay filter to produce the smooth profiles u1sg, u2sg, and u3sg (Fig. 2d).

The presence of the branch point causes the MNLMPC calculations to attain the Utopia solution, validating the analysis of Sridhar(2024)[18].

## II. CONCLUSIONS

Bifurcation analysis and multiobjective nonlinear control (MNLMPC) studies on a mastitis dynamic model. The bifurcation analysis revealed a branch point. The branch point (which causes multiple steady-state solutions from a singular point) is very beneficial because it enables the Multiobjective nonlinear model predictive control calculations to converge to the Utopia point (the best possible solution) in the models. A combination of bifurcation analysis and Multiobjective Nonlinear Model Predictive Control(MNLMPC) for a mastitis dynamic model is the main contribution of this paper.

*Data Availability Statement*

All data used is presented in the paper

*Conflict of interest*

The author, Dr. Lakshmi N Sridhar has no conflict of interest.

*Acknowledgement*

Dr. Sridhar thanks Dr. Carlos Ramirez and Dr. Suleiman for encouraging him to write single-author papers

## REFERENCES

1. Lam, T. J., M.C DeJong, Y.H Schukken, A.Brand, Mathematical modeling to estimate efficacy of post-milking teat disinfection in split-udder trials of dairy cows, J. Dairy Sci 79, 62-70 (1996).
2. Cherry,B. R., M.J Reeves, G. Smith, Evaluation of bovine viral diarrhea virus control using a mathematical model of infection dynamics, Prev. Vet. Med. 33, 91-108(1998).
3. Hamann,J., Diagnosis of Mastitis and Indicators of Milk Quality. In: Hogeveen, H. (Ed.) Proceedings of 4th IDF International Dairy Conference: Mastitis in Dairy Production- Current Knowledge and Future Solutions., Wageningen :Wageningen Academic Publishers. 82-90(2005).
4. Dorte, D., J. C Mike, F. M Graham, Modelling the dynamics of intramammary E. coli infections in dairy cows: understanding mechanisms that distinguish transient from persistent infections, Vet. Res. 41, 13(2010).
5. Michelle, B., L. H Jon, E. R Christine, J. R. Stephen, and J.S. Dov, Mathematical modelling of antimicrobial resistance in agricultural waste highlights importance of gene transfer rate, FEMS Microbiology Ecology 92 (2016).
6. Cobirka, M., V. Tancin, P. Slama, Epidemiology and classification of mastitis. Animals 2212. 10,12(2020) Nov26;.
7. Abera , A., . Review on prevalence and associated risk factors of bovine mastitis in lactating cows of small holder dairy farms in Ethiopia, Journal of Medical Research and Health Sciences 3, 5(2020).


©2025 Great Britain Journals Press

8. Izneid, B. A., Gurmu, E. D., Obsu, L. L., Melese, A. S., Kanan, M., & Al-Qerem, A. (2023). Optimal Control Strategy on Mathematical Model for the Dynamics of Mastitis. *Abstract and Applied Mathematics*, *17*(4), 699-711.
9. Dhooge, A., Govearts, W., and Kuznetsov, A. Y., MATCONT: "A Matlab package for numerical bifurcation analysis of ODEs", *ACM transactions on Mathematical software* 29(2) pp. 141-164, 2003.
10. Dhooge, A.,W. Govaerts; Y. A. Kuznetsov, W. Mestrom, and A. M. Riet , "CL_MATCONT"; *A continuation toolbox in Matlab,* 2004.
11. Kuznetsov,Y.A. "Elements of applied bifurcation theory" .*Springer,*NY, 1998.
12. Kuznetsov,Y.A.(2009)."Five lectures on numerical bifurcation analysis" ,*Utrecht University,*NL., 2009.
13. Govaerts, w. J. F., "Numerical Methods for Bifurcations of Dynamical Equilibria", *SIAM*, 2000.
14. Flores-Tlacuahuac, A. Pilar Morales and Martin Riveral Toledo; "Multiobjective Nonlinear model predictive control of a class of chemical reactors" . *I & EC research*; 5891-5899, 2012.
15. Hart, William E., Carl D. Laird, Jean-Paul Watson, David L. Woodruff, Gabriel A. Hackebeil, Bethany L. Nicholson, and John D. Siirola. "Pyomo – Optimization Modeling in Python" Second Edition. Vol. 67.
16. Wächter, A., Biegler, L. "On the implementation of an interior-point filter line-search algorithm for large-scale nonlinear programming". *Math. Program.* 106, 25–57 (2006). https://doi.org/10.1007/s10107-004-0559-y
17. Tawarmalani, M. and N. V. Sahinidis, "A polyhedral branch-and-cut approach to global optimization", *Mathematical Programming*, 103(2), 225-249, 2005
18. Sridhar LN. (2024)Coupling Bifurcation Analysis and Multiobjective Nonlinear Model Predictive Control. Austin Chem Eng. 2024; 10(3): 1107.
19. Upreti, Simant Ranjan(2013); Optimal control for chemical engineers. Taylor and Francis.

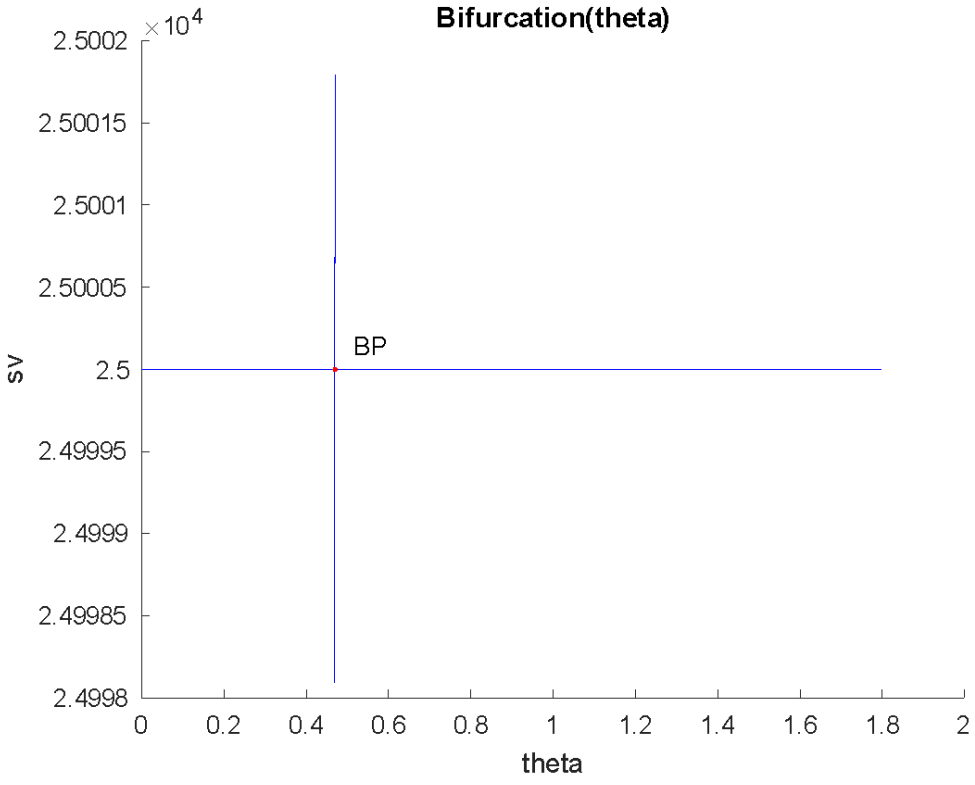


*Fig. 1a* $\theta$*:* Is bifurcation parameter





©2025 Great Britain Journals Press

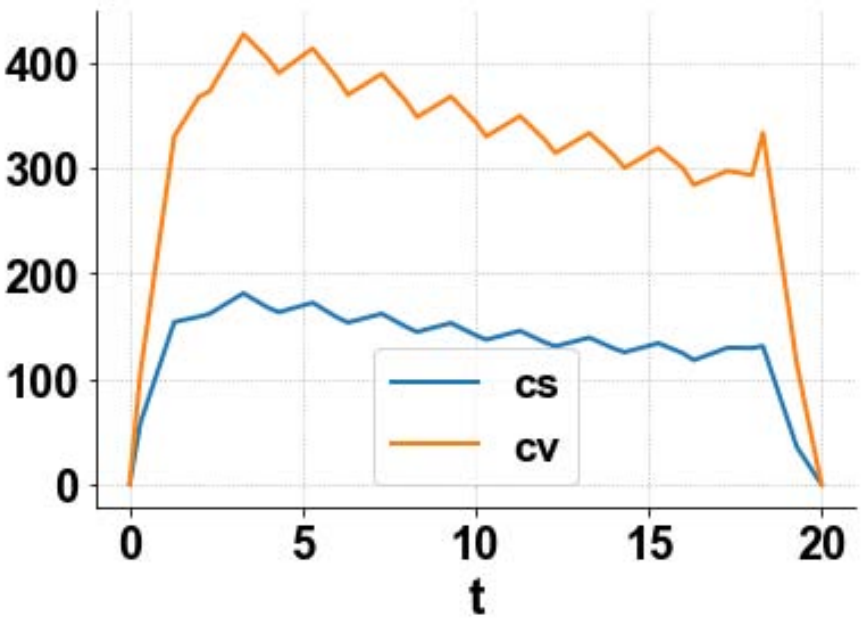


*Fig. 2a:* MNLMPC cs, cv profiles

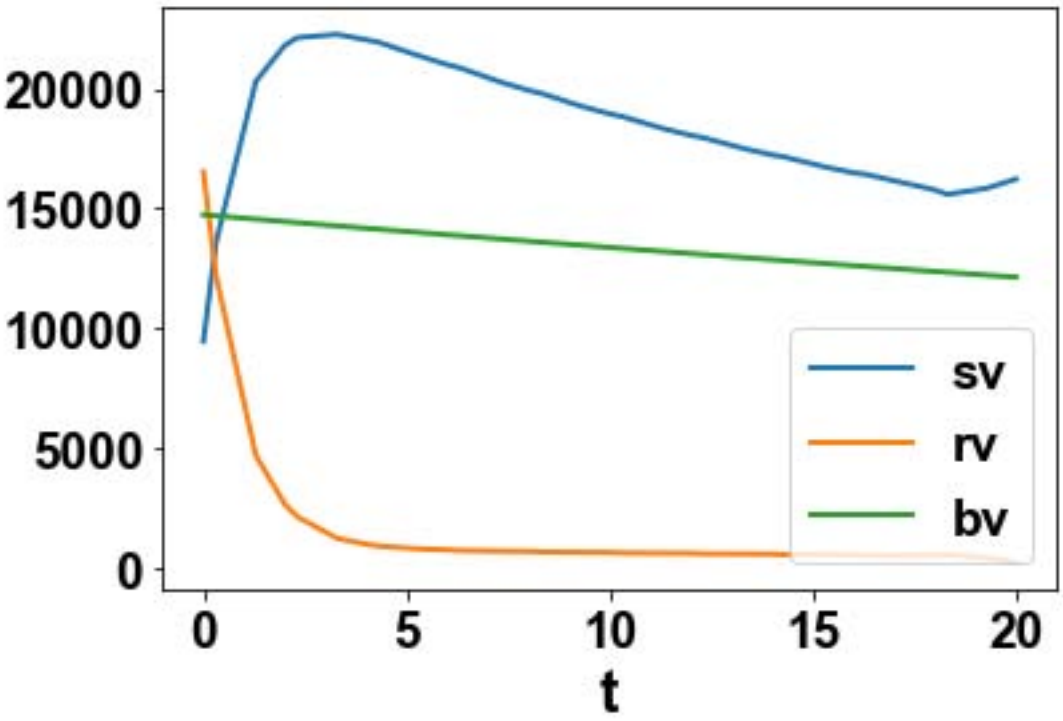


*Fig. 2b:* MNLMPC sv, rv,bv profiles


©2025 Great Britain Journals Press

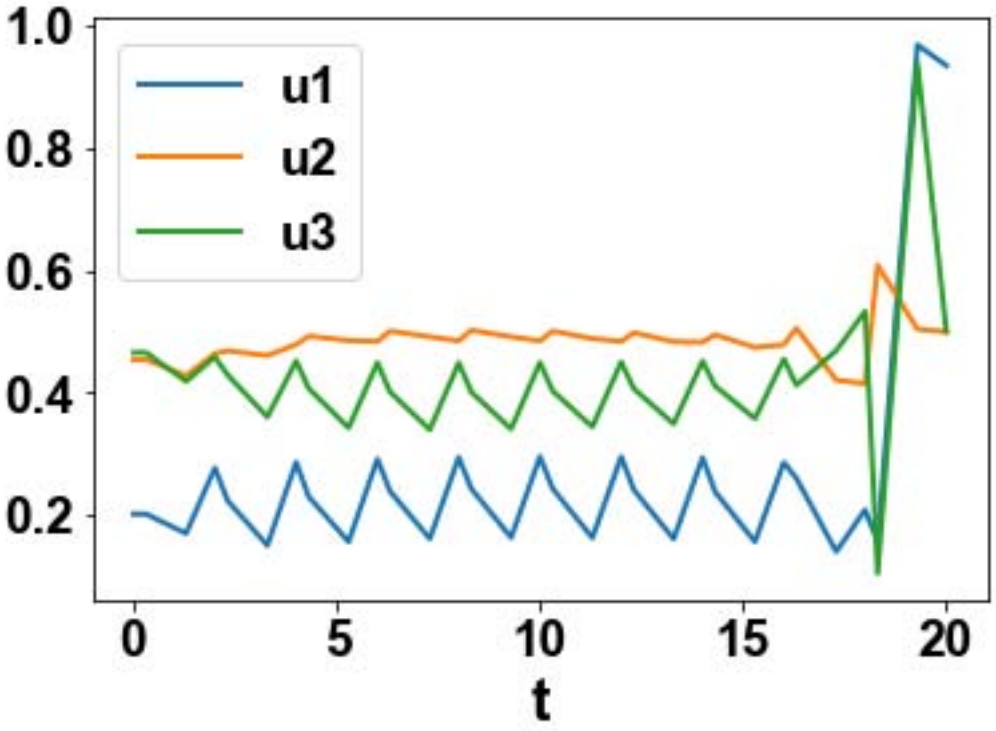


*Fig. 2c:* MNLMPC u1, u2, u3 profiles

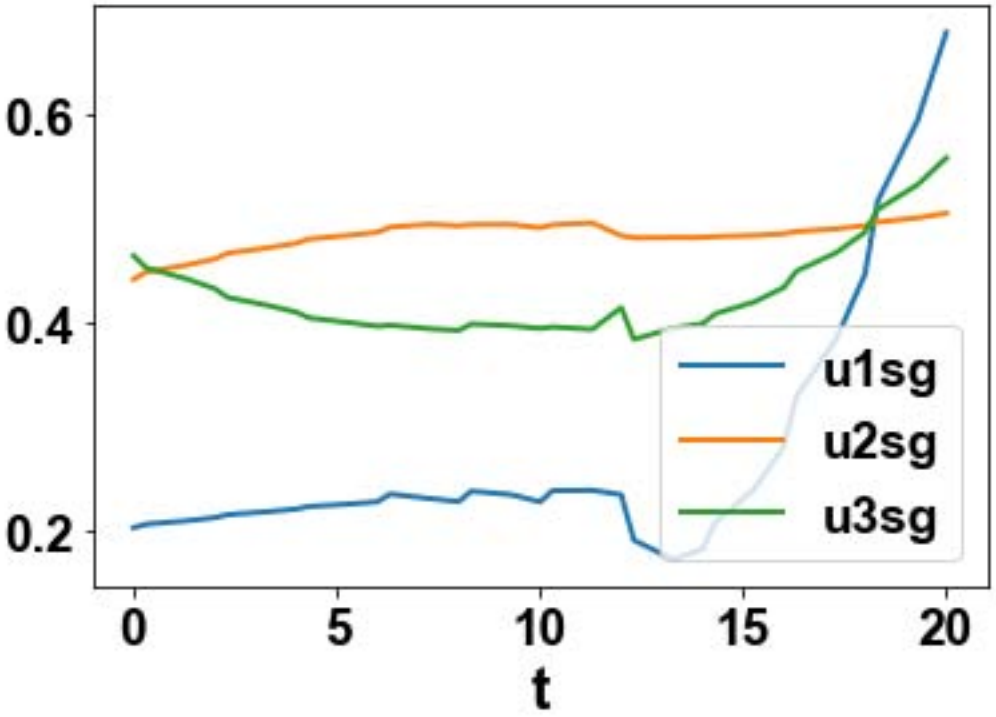


*Fig. 2d:* MNLMPC u1sg, u2sg, u3sg profiles





©2025 Great Britain Journals Press